

# G PROTEIN MECHANISMS: Insights from Structural Analysis

*Stephen R. Sprang*

Howard Hughes Medical Institute and Department of Biochemistry,  
The University of Texas Southwestern Medical Center, Dallas, Texas 75235-9050;  
e-mail: sprang@howie.swmed.edu

KEY WORDS: G proteins, Ras-like proteins, elongation factors, protein tertiary structure, receptors

---

## ABSTRACT

This review is concerned with the structures and mechanisms of a superfamily of regulatory GTP hydrolases (G proteins). G proteins include Ras and its close homologs, translation elongation factors, and heterotrimeric G proteins. These proteins share a common structural core, exemplified by that of p21<sup>ras</sup> (Ras), and significant sequence identity, suggesting a common evolutionary origin. Three-dimensional structures of members of the G protein superfamily are considered in light of other biochemical findings about the function of these proteins. Relationships among G protein structures are discussed, and factors contributing to their low intrinsic rate of GTP hydrolysis are considered. Comparison of GTP- and GDP-bound conformations of G proteins reveals how specific contacts between the  $\gamma$ -phosphate of GTP and the switch II region stabilize potential effector-binding sites and how GTP hydrolysis results in collapse (or reordering) of these surfaces. A GTPase-activating protein probably binds to and stabilizes the conformation of its cognate G protein that recognizes the transition state for hydrolysis, and may insert a catalytic residue into the G protein active site. Inhibitors of nucleotide release, such as the  $\beta\gamma$  subunit of a heterotrimeric G protein, bind selectively to and stabilize the GDP-bound state. Release factors, such as the translation elongation factor, Ts, also recognize the switch regions and destabilize the Mg<sup>2+</sup>-binding site, thereby promoting GDP release. G protein-coupled receptors are expected to operate by a somewhat different mechanism, given that the GDP-bound form of many G protein  $\alpha$  subunits does not contain bound Mg<sup>2+</sup>.

---

## CONTENTS

PERSPECTIVE .....	640
TERTIARY STRUCTURES OF G PROTEINS .....	641

<i>The GTPase Fold</i> .....	641
<i>Ras and Its Homologs</i> .....	643
<i>Translation Elongation Factors</i> .....	647
<i>Heterotrimeric G Protein <math>\alpha</math> Subunits</i> .....	648
GUANINE NUCLEOTIDE RECOGNITION .....	650
STRUCTURAL CHANGES UPON GTP BINDING: EFFECTOR RECOGNITION .....	654
<i>Ras-Effector Interactions</i> .....	655
<i>The Complex of Elongation Factor Tu with Amino-Acyl tRNA</i> .....	656
<i>Effector Interactions with <math>G_{\alpha}</math> Subunits</i> .....	657
MECHANISM OF GTP HYDROLYSIS .....	659
MECHANISM OF CATALYTIC RATE ENHANCEMENT BY GAP .....	663
REGULATION OF GUANINE NUCLEOTIDE EXCHANGE .....	665
<i><math>\beta\gamma</math> Subunits of Heterotrimeric G Proteins</i> .....	665
<i>GEFs of the Ras Family</i> .....	670
<i>Elongation Factor Ts</i> .....	672
SUMMARY .....	672

## PERSPECTIVE

G proteins are a superfamily of regulatory GTP hydrolases. Available crystal structures, which are discussed in detail in this review (see also 1a), demonstrate that all members of this group share a common structural core, exemplified by that of p21<sup>ras</sup> (Ras). This structural similarity is reflected in significant sequence identity, suggesting a common evolutionary origin for these proteins (1, 2). Unlike efficient catalysts, G proteins form relatively stable complexes with their substrate, GTP, and product, GDP. G proteins have a conserved recognition site for guanine nucleotides, although mechanisms of GTP hydrolysis differ in detail. In all G proteins, binding and hydrolysis of GTP triggers reciprocal conformational changes within a switch region within the catalytic domain. The GTP- and GDP-bound complexes define, respectively, the active and inactive states of a G protein as a regulatory molecule. There are many variations on this theme. The transition between active and inactive states may be limited by the intrinsic rate of GTP hydrolysis, or it may be accelerated by the binding of a GTPase-activating protein (GAPs) or by association of the G protein with a particular conformational state of its cognate target (effector). Thus, within the G protein superfamily are found clocks (heterotrimeric G protein  $\alpha$  subunits), switches or adapters (Ras and its homologs), and sensors (translation elongation factors, Tu and G). Guanine nucleotide dissociation inhibitors (GDIs) inhibit the release of GDP from certain G proteins, whereas guanine nucleotide exchange or release factors (GEFs) stimulate this process. These factors that control G protein state may themselves be subject to regulation. The participation of such accessory molecules expands in scope and intricacy the basic G protein regulatory paradigm. The mechanisms of G protein activity and regulation with respect to this paradigm are discussed in relation to the three-dimensional structures of these molecules.

Much of our present understanding of the mechanism of G protein action has come from biochemical and structural, particularly X-ray crystallographic, investigations. The extent to which three-dimensional structures of G proteins have illuminated their biochemical and cellular activities is highlighted in this review. The focus here is on the three most thoroughly studied G protein groups: Ras and its homologs; the translation elongation factors, Tu and G (EF-Tu, EF-G); and the  $\alpha$  subunits ( $G_\alpha$ ) of heterotrimeric G proteins. The roles of these molecules in cellular metabolism and their physiological function in cells or tissues is not discussed. Instead, questions that bear most directly on the chemical and conformational mechanisms by which G proteins interact with their targets and regulators are addressed. How are the structures of G proteins related? What structural characteristics account for their remarkably low but physiologically useful rate of GTP turnover? By what mechanisms do GAPs accelerate GTP hydrolysis? How do GTP and GDP enforce different conformational states, and how are these states coupled to effector recognition? How do GDIs (such as the  $\beta\gamma$  subunit of a heterotrimeric G protein) prevent, or how does a GEF (such as EF-Ts or a heterotrimeric G protein-coupled receptor) catalyze GDP release, thereby regulating the rate at which G proteins are interconverted from their basal state to their activated state?

## TERTIARY STRUCTURES OF G PROTEINS

### *The GTPase Fold*

At the core of every G protein is a guanine nucleotide-binding domain first described at low resolution nearly 20 years ago in the three-dimensional structure of a proteolytically modified, GDP-bound form of EF-Tu from *Escherichia coli* (3, 4). Crystallographic analyses at higher resolution (5, 6) revealed a 200-residue domain consisting of a central six-stranded  $\beta$ -sheet surrounded by  $\alpha$ -helices (Figure 1). Structurally, the G protein fold is a variation upon the classical nucleotide-binding fold (7). The five polypeptide loops that form the guanine nucleotide-binding site are the most highly conserved elements in this domain and define the G protein superfamily (Figure 2). The five loops are designated G-1 through G-5 (Table 1) (2); the primary structures of three of the loops, G-1, G-3, and G-4, conform to sequence templates (8) that are well conserved in and diagnostic of EF-Tu, p21<sup>ras</sup> (5, 9, 10), and  $G_\alpha$  subunits (11).

The diphosphate-binding loop (P-loop or G-1 box) with the consensus sequence, GXXXXGK(S/T), connects the  $\beta$ 1 strand to the  $\alpha$ 1 helix (Figure 1) and contacts the  $\alpha$ - and  $\beta$ -phosphates of the guanine nucleotide (Figure 2). The primary structure of the G1 loop places it within a larger family of phosphate-binding sequences (12) found in other nucleotide-binding proteins. A DXXG sequence, G-3, at the N terminus of the  $\alpha$ 2 helix links the subsites for binding of  $Mg^{2+}$  and the  $\gamma$ -phosphate of GTP. The G1 and G3 sequences correspond,

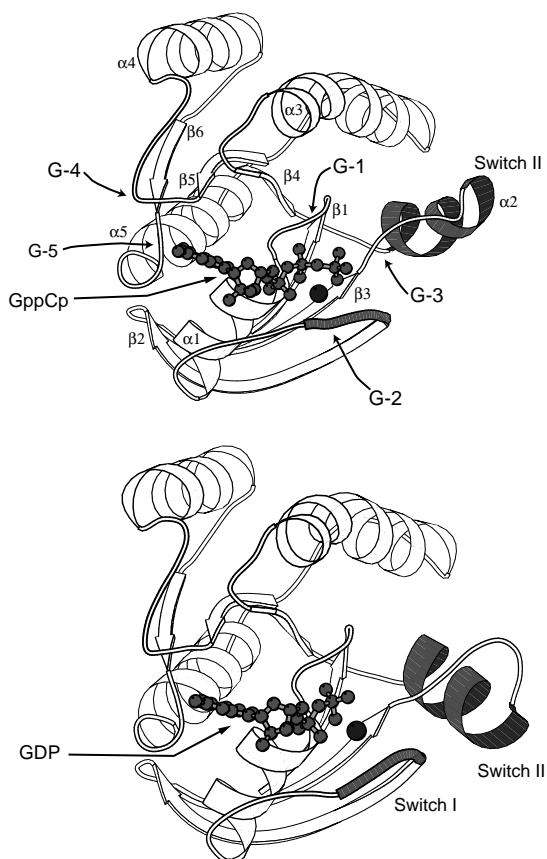


*Figure 1* A schematic diagram of Ras; switch segments are darkened, secondary structure elements and G-box (2) regions are labeled. *Top*: The GppCp · Mg<sup>2+</sup> complex, coordinates taken from Protein Databank (PDB) entry 5P21 (235). The nonhydrolyzable GTP analog is depicted by a ball-and-stick model. The single solid sphere represents Mg<sup>2+</sup>. *Bottom*: The GDP complex (PDB entry 4Q21). All figures were drawn with the computer program Molscript (234).

respectively, to the Walker A and Walker B boxes (13) found in many nucleotide-binding proteins, many of which (viz myosin, sugar kinases, transport ATPases, and ATP synthetases) are not G protein homologs. The guanine ring is recognized, in part, by the conserved NKXD sequence (G-4) that links the  $\beta 5$  strand and the  $\alpha 4$  helix. The connection (G-2) between the  $\alpha 1$  helix and the  $\beta 2$  strand contains a conserved threonine residue involved in Mg<sup>2+</sup> coordination. The G-5 box, located between  $\beta 6$  and helix  $\alpha 5$  with consensus sequence (T/G)(C/S)A,

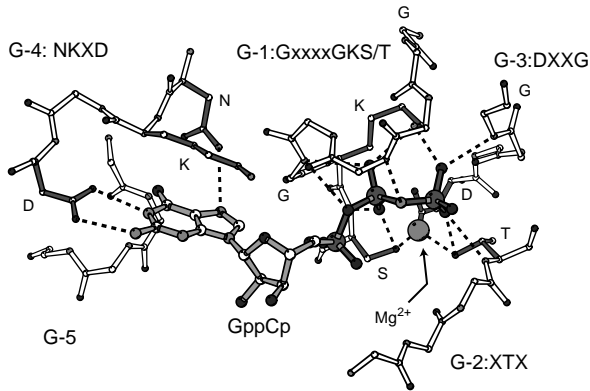


Figure 2 The guanine nucleotide binding site of Ras in the GppCp · Mg<sup>2+</sup> complex: Side chains of the highly conserved G-box residues are darkened and labeled with the one-letter amino acid code.

buffers the guanine base recognition site. The G-box nomenclature is used hereafter in the text to refer to elements of the guanine nucleotide-binding site or residues located within them. Similarly, the term G domain denotes the entire Ras-like or GTPase domain that is the conserved core in all G proteins. Unless otherwise noted, stereochemical descriptions are based on the most highly refined X-ray structures available for: human Ras · Mg<sup>2+</sup> · GppNp (14); Ras · Mg<sup>2+</sup> · GDP (15); EF-Tu · Mg<sup>2+</sup> · GppNp from *Thermus aquaticus* (16) and *Thermus thermophilus* (17); *T. aquaticus* EF-Tu · Mg<sup>2+</sup> · GDP (18a); bovine transducin  $\alpha$  (G<sub>1 $\alpha$</sub> ) · GTP $\gamma$ S · Mg<sup>2+</sup> (19) and G<sub>1 $\alpha$</sub>  · GDP · Mg<sup>2+</sup> (20); and the  $\alpha$  subunit of the inhibitory (for adenylyl cyclase) G protein, G<sub>i</sub>, from the rat (G<sub>i $\alpha$ 1</sub>) · GTP $\gamma$ S · Mg<sup>2+</sup> (21) and G<sub>i $\alpha$ 1</sub> · GDP (22).

### *Ras and Its Homologs*

Ras, an important regulator of cell proliferation, is an essential component of signal transduction pathways initiated by receptor-tyrosine kinases. Homologs of Ras regulate a variety of processes essential for cytoskeletal remodeling, differentiation, and vesicle transport (see 1, 23–26 for reviews). As predicted (5, 10), the guanine-nucleotide binding domain of EF-Tu (Figure 3) proved to be a good model for the corresponding domain of Ras (27, 28). Most crystallographic studies of Ras have used a truncated form of human p21<sup>H-ras</sup> containing the N-terminal 171 (15, 27, 29–31) or 166 residues (14, 28, 32–34). The truncated Ras proteins possess normal GTPase activity (29, 35). The structure of the intact 189-residue p21<sup>H-ras</sup> indicates that the C-terminal residues are poorly ordered (30). A series of posttranslational modifications,

**Table 1** Conserved nucleotide binding motifs in selected G-proteins<sup>a</sup>

Protein	G-1	G-2	G-3	G-4	G-5
H Ras	10 GAGVGGS	32 YPDTIED	55 I LDTAGQE	114 VGKCD	142 YIETSAK
H Rap-1A	10 GSGVGGS	32 YDPTIED	55 I LDTAGTE	114 VGKCD	140 FLGSSAK
H Ran	17 GDGGTGKS	40 YVATLGV	63 NWDTAGQE	120 CGNKVD	146 YIETSAK
H ARF-1A	24 GLGAAGKT	45 T I P T I G F	65 VWDVGGQD	124 FANKQD	155 IQATCAT
Ec EF-Tu	18 GHVDHGKT	58 R G I T I N T	79 H V D G P G H A	133 F L N K C D	169 I V R G S A L
Tt EF-G	19 AHIDAGKT	61 R G I T I T A	81 I I D T P G H V	135 F A N K M D	258 V F L G S A L
B G <sub>α</sub>	47 GAGESGKS	201 R V L T S G I	221 M F D V G G Q R	290 F L N K Q D	361 P H F T C A V
B G <sub>1α</sub>	40 GAGESGKS	178 R V K T T G I	198 L F D V G G Q R	267 F L N K K D	321 T H F T C A T
B G <sub>2α</sub>	36 GAGESGKS	174 R V K T T G I	194 M F D V G G Q R	263 F L N K K D	317 S H M T C A T
B G <sub>3α</sub>	40 GAGESGKS	179 R V K T T G I	199 M F D V G G Q R	268 F L N K K D	321 C H M T C A T
H G <sub>α</sub>	40 GTSNSGKS	179 R D M I T G I	199 M V D V G G Q R	268 F L N K K D	322 S H F T C A T
M G <sub>α</sub>	40 GTGESGKS	177 R V P T T G I	197 M V D V G G Q R	266 F L N K K D	320 S H F T C A T

<sup>a</sup>Sequences compiled from (2) and (19) for all but Rap-1a (39), Ran (40a) and ARF-1A (42). Numbers preceding the sequences correspond to the first residue number of the motif. Species origin of sequences are designated as follows: H, human; B, bovine; M, Mouse; EC, *E. coli*; Tt, *T. thermophilus*.

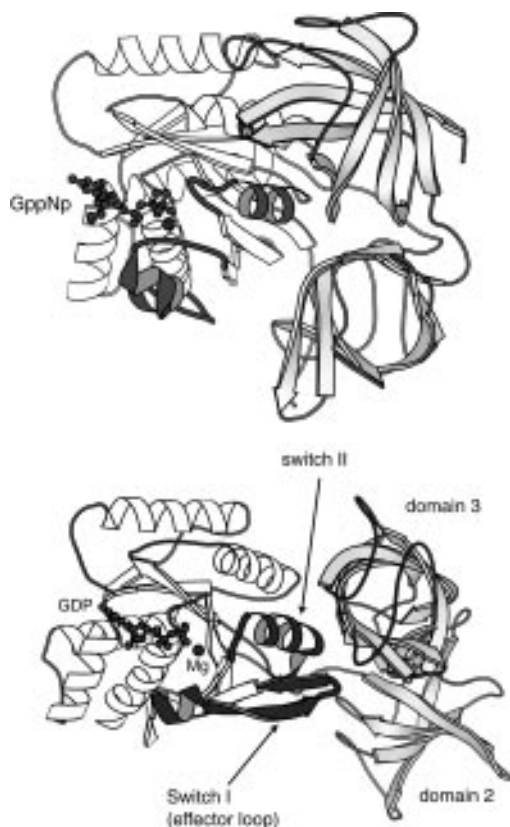


*Figure 3* The structure of Elongation Factor Tu from *T. aquaticus* is shown in the GppNp · Mg<sup>2+</sup>-bound conformation (16) (PDB entry 1EFT) (*top*) and in the complex with GDP · Mg<sup>2+</sup> (18a) (PDB entry 1TUI; M Kjeldgaard, personal communication). Switch regions are labeled, and domains 2 and 3 are highlighted in gray. The nucleotide-Mg<sup>2+</sup> complexes are depicted as in Figure 1.

including isoprenylation and carboxymethylation of Cys-186, are required to localize p21<sup>H-ras</sup> to the plasma membrane (reviewed in 36).

The prototypical G protein, Ras possesses the minimal apparatus necessary both to catalyze GTP hydrolysis (albeit inefficiently) and to convert the resulting free energy change into a conformational transition that facilitates its dissociation from effector. A comparison of the Ras · GDP · Mg<sup>2+</sup> complex (15) with the Mg<sup>2+</sup> complexes of Ras harboring the nonhydrolyzable analogs GppNp (14) [guanosine-5'-( $\beta,\gamma$ -imido)-triphosphate] or GppCp [guanosine-5'-( $\beta,\gamma$ -methylene) triphosphate] (30) shows that two regions of Ras change conformation upon GTP hydrolysis. One of these regions, designated switch I

(Figure 1), corresponds to the G-2 loop that forms part of the  $Mg^{2+}$ -binding site. This segment has been implicated in both effector and Ras-GAP binding (37) and is therefore called the effector loop (28). The second mobile segment, called switch II, encompasses G-3 (which forms the GTP  $\gamma$ -phosphate binding site) and the  $\alpha 2$  helix that follows (Figure 1). Structures, even of the same nucleotide complex, determined from different crystal forms show considerable variation in the conformation of switch II (30), suggesting that crystal packing forces can influence the structure of Ras in the switch II region. High resolution solution structures of the Ras  $\cdot$   $Mg^{2+}$   $\cdot$  GDP complex determined by nuclear magnetic resonance (NMR) reveal a switch II conformation slightly different from those defined in the solid state (38) and also show that both G-1 and G-3 are flexible on the nanosecond time scale. Thus, the conformation of the switch regions appears to be inherently unstable, indicating that these structural elements are malleable.

The molecular architecture of Ras is recapitulated in the structures of other small G proteins: Rap1a, a competitive inhibitor of Ras (determined in the GppCp form as a complex with the Ras-binding domain of Raf-1) (39); Ran  $\cdot$  GDP  $\cdot$   $Mg^{2+}$  (40a); and the ADP-ribosylation factor 1 (ARF-1) complex with GDP (41, 42). Ran, a 216-residue protein that is involved in nuclear protein import (see references cited in 40), bears only 12% sequence identity to Ras but adopts essentially the same tertiary fold. However, the crystal structure of human Ran  $\cdot$  GDP  $\cdot$   $Mg^{2+}$  determined at 2.3 Å resolution shows that the structure terminates in a well-ordered  $\beta 7$  strand and a C-terminal helix that is not present in Ras. Further, the  $\alpha 1$  helix is split into two smaller helices ( $\alpha 1a$  and  $\alpha 1b$ ). The effector loop that follows is consequently displaced from the position it occupies in Ras and adopts an alternative conformation as the short beta strand  $\beta 2_E$ . Antiparallel to strand  $\beta 2$ , the effector loop forms a beta hairpin in Ran. Also as a consequence of altered effector loop conformation, the G-2 threonine residue (Table 1) of Ran cannot serve as an  $Mg^{2+}$  ligand, as do the corresponding residues in Ras. In this respect, the GDP  $\cdot$   $Mg^{2+}$  complex of Ran is similar to that of *T. aquaticus* EF-Tu (18a). Also in contrast to Ras, both switch regions of Ran are well ordered.

The 181-residue ARF-1 protein was originally identified as a cofactor required for cholera toxin-mediated ADP ribosylation of the  $\alpha$  subunit of the stimulatory (for adenylyl cyclase) G protein,  $G_s$  (43), but more recently has been shown to be a component of the vesicle budding apparatus in the Golgi body (44), and a coactivator of phospholipase D (45). ARF-1 cycles from the cytosol in its GDP  $\cdot$   $Mg^{2+}$ -bound state to a coatomer-associated protein complex bound on the vesicle membrane in its GTP-bound state. Structures of human ARF-1  $\cdot$  GDP  $\cdot$  M (M =  $Mg^{2+}$  or  $Ca^{2+}$ ) (41), and the corresponding complex of rat ARF-1 (42), have been determined at 2.0 and 2.6 Å resolution, respectively.

The tertiary fold of ARF-1, which is only 11% identical in primary structure to Ras, differs from the latter in three respects. First, like Ran, the effector loop of Arf-1 adopts a  $\beta$  conformation ( $\beta_{2E}$ ). Moreover, in all three crystal forms reported, ARF-1 forms a dimer, in which two molecules associate by an antiparallel hydrogen-bonding interaction between the  $\beta_{2E}$  strands, thereby forming a continuous 14-stranded  $\beta$ -sheet and suggesting a mechanism for effector engagement (41). In one of the two crystal forms of rat ARF-1 (42), the antiparallel contacts between  $\beta_{2E}$  strands at the dimer interface are much less extensive. Second, in the structure of ARF-1 there is an amphipathic N-terminal  $\alpha$  helix that is not present in Ras (but is reminiscent of a similar element in  $G_{i\alpha 1}$ ). Finally, the DVGG sequence in G-3 of ARF-1 (Table 1) is displaced two residues relative to the position of the corresponding sequence in Ras, a difference which, it has been speculated, may account for the very low intrinsic GTPase activity of ARF-1 (41).

Upon comparing the structures of Ras and its homologs, it becomes clear that the nucleotide  $\alpha$ - and  $\beta$ -phosphate recognition loop (G-1) and the guanine base recognition loop (G-4) are remarkably similar in structure, whereas the  $Mg^{2+}$  (G-2) and GTP  $\gamma$ -phosphate-binding site (G-3)—the switch regions—differ.

### *Translation Elongation Factors*

The GTP-bound form of EF-Tu delivers aminoacyl-tRNA (AA-tRNA) to a complementary codon on the ribosome, while EF-G catalyzes translocation of mRNA by one codon along the ribosome and transfer of the peptidyl-tRNA from the A to the P site (46). In EF-Tu (Figure 3), the Ras-like (G) domain is tethered by a flexible linker to a tandem pair of antiparallel  $\beta$  barrel domains (domains 2 and 3) that each comprise about 90 residues and have a “greek key” fold (18). Domains 2 and 3 are connected to each other by a short but extended linker peptide yet are in close contact. The long axes of the  $\beta$  barrels of domains 2 and 3 are nearly orthogonal. In the  $GDP \cdot Mg^{2+}$  complex of *E. coli* EF-Tu (18), the G domain is spatially separated from domain 2 but closely associated with domain 3 (Figure 3, *bottom*). Due to this unusual organization, the protein contains a large solvent channel bounded by the G domain and domain 2 and the linker between them. The first crystals of the *E. coli*  $GDP \cdot Mg^{2+}$  complex could only be obtained after mild proteolysis, which results in the excision of the G-2/effector loop, the site at which EF-Tu interacts with the ribosome (47). In the intact *T. aquaticus* EF-Tu  $\cdot$  GDP complex (Figure 2) (18a), and in an intact form of *E. coli* EF-Tu complexed with  $GDP \cdot Mg^{2+}$  (47b), the effector loop adopts an extended  $\beta$  hairpin conformation, similar to that in Ran and ARF-1, that protrudes into domain 2. The numbering convention used here for EF-Tu residues refers to the *E. coli* enzyme. GTP binding drastically changes the secondary structure of the effector loop and causes a massive and coordinated

rearrangement of the positions of domains 2 and 3 relative to the G domain, thereby creating a binding site for AA-tRNA (16, 17), as described in greater detail below.

The X-ray structure of EF-G has been determined in both the nucleotide-free (48) and GDP-bound (49) forms at 2.85 and 2.7 Å resolution, respectively. The architecture of the first two domains of EF-G is roughly similar to that of EF-Tu, but EF-G contains three other domains not present in EF-Tu. As in EF-Tu, the G domain of EF-G is located at the N terminus of the molecule. However, in contrast to other G proteins, the G domain is expanded by a 90-residue  $\alpha+\beta$  subdomain inserted between helix  $\alpha 4$  and strand  $\beta 6$ . The second domain is a nine-stranded  $\beta$  barrel, considerably larger than that in EF-Tu. Remarkably, the placement of domain 2 of EF-G with respect to its G domain is similar to that in the  $\text{GTP} \cdot \text{Mg}^{2+}$  complex of EF-Tu, rather than in the GDP-bound form. EF-G has no analog to the third domain of EF-Tu but instead possesses three additional domains, all  $\alpha$ - $\beta$  sandwiches. The third and fifth domains are similar to each other and resemble the structure of ribosomal protein, S6. Domain 5 occupies a position similar to that of domain 3 in EF-Tu. The fourth domain, which forms the tip of the molecule furthest from the G domain, contains an unusual left-handed  $\beta\alpha\beta$  crossover connection and is similar in structure to the ribosomal protein S5. The GDP-bound and unliganded structures of EF-G, which are similar, bear a remarkable resemblance to the complex of  $\text{GTP} \cdot \text{Mg}^{2+}$ -bound EF-Tu with tRNA (50). The footprint of the three ribosomal protein-like domains in EF-G is highly reminiscent of the space occupied by tRNA in the EF-Tu complex. Thus, the GDP-bound form of EF-G may bind to a ribosomal site similar to that occupied by the GTP-bound form of EF-Tu/AA-tRNA (see 46, 50, 51 for discussion).

### *Heterotrimeric G Protein $\alpha$ Subunits*

More than 20 different mammalian G protein  $\alpha$  subunits have been identified, corresponding to 16 gene products divided into four active major classes:  $\alpha_{s(\text{olf})}$ ,  $\alpha_{i(\text{o,t,g,z})}$ ,  $\alpha_q(11,14-16)$ , and  $\alpha_{12(13)}$  (189). G proteins are activated by cell-surface receptors of the seven-transmembrane-helix class, which catalyze the exchange of GDP for GTP in the guanine nucleotide-binding site of the  $\alpha$  subunit. When bound to GTP,  $G_\alpha$  subunits can regulate intracellular effectors, such as adenylyl cyclase, phospholipase  $C\beta$ ,  $\text{K}^+$  and  $\text{Ca}^{2+}$  channels, and cyclic GMP phosphodiesterases. In the GDP-bound state,  $G_\alpha$  subunits are inhibited by binding to a heterodimer composed of the  $G_\beta$  and  $G_\gamma$  subunits (hereafter referred to as  $\beta\gamma$ ), which are released upon receptor-mediated nucleotide exchange (for reviews see 11, 52–56). The architectures of  $G_{i\alpha}$  (19) and  $G_{i\alpha 1}$  (21) are likely to be typical of all members of the G protein  $\alpha$  subunit family (Figure 4). Relative

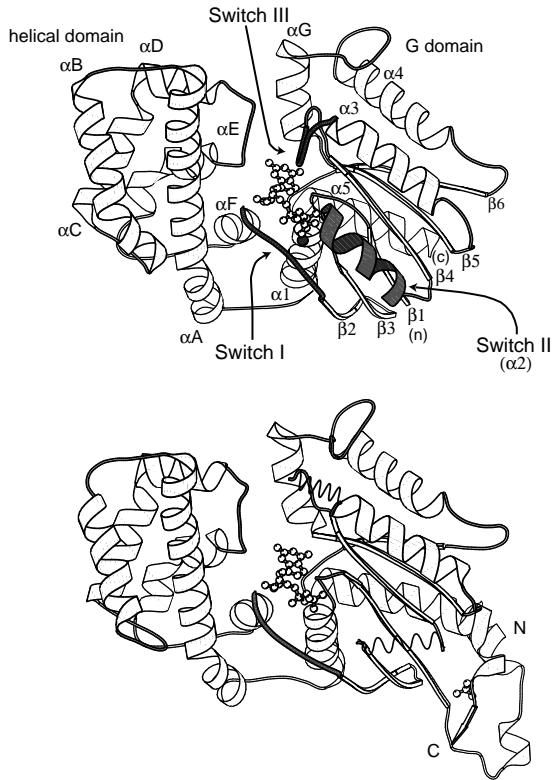


*Figure 4* Top:  $G_{i\alpha 1}$  in the  $GTP\gamma S \cdot Mg^{2+}$  complex (21) (PDB entry 1GIA), with switch segments darkened and secondary structure elements labeled. (n) and (c) mark the positions at which the N- and C-termini become ordered in the crystal structure (residues 33 and 343, respectively). In the GDP complex (22) (PDB entry 1GDD), switches II and III are disordered, whereas the amino terminus N, from residue 8, and the carboxy terminus C, residue 354, are ordered. The nucleotide- $Mg^{2+}$  complexes and a bound sulfate ion are depicted as in Figure 1.

to the core of Ras,  $G_{\alpha}$  subunits are interrupted by four insertions. The largest of these is interposed between helix  $\alpha 1$  and strand  $\beta 2$ , just N-terminal to the  $Mg^{2+}$ -binding site (G-2). The insertion folds into a six-helix bundle, which could be viewed as an antiparallel four-helix bundle that is distorted by a kink in the last helix and terminated by a short helical segment. This helical bundle insertion is in fact an independently folded domain: The corresponding fragment from  $G_{s\alpha}$  can be expressed as a recombinant protein (57), associates with the heterologously expressed G domain of  $G_{s\alpha}$ , and possesses an ordered

three-dimensional structure that is similar to the corresponding domains in intact  $G_{i\alpha 1}$  and  $G_{t\alpha}$  (58). The structures of the helical domains of  $G_{t\alpha}$ ,  $G_{i\alpha 1}$ , and  $G_{s\alpha}$  differ only in the orientation of the second helix and the following interhelical loop (B helix and B/C loop). Postulated roles for the helical domain, include increasing the affinity of GTP binding (19), acting as a tethered intrinsic GAP (57, 59, 60), and participating in effector recognition (22, 58, 61) (see below). Two major splice variants of  $G_{s\alpha}$  have been identified (11); the longer of these contains an additional 13 residues inserted N-terminal to the first helical segment (helix A) of the helical domain. Other insertions present in  $G\alpha$  subunits that are absent in the Ras core include: an Asp/Glu-rich loop extending the  $\beta 4$ -strand-helix- $\alpha 3$  connection (and buttressing the helical domain); a 20-residue extension of the  $\beta 5$  strand (30 in  $G_{s\alpha}$ ) that folds into a helix ( $\alpha G$ )-loop segment following G-4; and a short extension of the loop connecting helix  $\alpha 4$  and strand  $\beta 6$ , preceding G-5. In addition, compared to Ras,  $\alpha$  subunits are extended at their N termini by 26–36 residues that, in  $G_{i\alpha 1}$  and  $G_{t\alpha}$ , can assume a disordered conformation or fold into a compact domain or into an extended  $\alpha$ -helix (see below), such as seen in ARF-1. The interface between the helical domain and the G domain creates a narrow crevice within which the guanine nucleotide is bound, although most of the GTP or GDP contacts are made with the five loops of the G domain.

Most  $G\alpha$  subunits (excluding  $\alpha_t$ ) are S-palmitoylated at a cysteine (or cysteines) near the amino terminus (62–64), and others ( $\alpha_o$ ,  $\alpha_i$ ,  $\alpha_z$ , and  $\alpha_t$ ) are N-myristoylated at Gly-2 as well (Met-1 is removed by posttranslational processing) (65, 66). These lipid modifications help tether  $\alpha$  subunits to the plasma membrane, juxtaposing them to their cognate receptors and effector targets (63). Addition and removal of the palmitoyl group appear to be dynamic receptor-mediated processes that may contribute to recycling of  $G\alpha$  between the membrane and cytosolic compartments (67, 68; for reviews see 69, 70). Members of the  $G_{\alpha i}$  family (excluding  $G_{\alpha z}$ ) can be ADP-ribosylated by pertussis toxin at a cysteine residue four residues removed from the C-terminus, thereby inhibiting interaction with their receptors (2, 11).  $G_{s\alpha}$  and  $G_{t\alpha}$  can be ADP-ribosylated at a conserved arginine in the G-2 box (Arg-201 in  $G_{s\alpha}$ ), which permits GTP binding but abolishes GTPase activity (59, 71).

## GUANINE NUCLEOTIDE RECOGNITION

In all G proteins studied so far, GTP is bound as a complex with  $Mg^{2+}$ , which is coordinated to one oxygen from the  $\beta$ -phosphate and one from the  $\gamma$ -phosphate (Figure 2). Although nucleotide-free Ras can be prepared (72), many G proteins, including Ras (73, 74) and particularly  $G\alpha$  subunits (75), are unstable in the absence of bound nucleotide. Hence, nucleotide affinities are estimated

from rates of nucleotide dissociation (76). For Ras, these rates are on the order of  $10^{-4}$  and  $10^{-5}$   $s^{-1}$  for GDP and GTP, respectively, in the presence of  $Mg^{2+}$  (73). When combined with the rate of association of nucleotide with Ras apoprotein, these kinetic values correspond to a dissociation constant of  $\sim 10^{-11}$  M. The affinity of EF-Tu (*T. thermophilus*) for GDP and GTP is also in the nanomolar range (77), with dissociation rates of  $10^{-3}$   $s^{-1}$  and  $10^{-2}$ , respectively (78); in this case, GDP actually binds more tightly than GTP. Off-rates of GTP from  $G_{o\alpha}$  (79) and  $G_{i\alpha 1}$  (80), determined in the presence of at least micromolar concentrations of  $Mg^{2+}$ , are less than  $10^{-3}$   $s^{-1}$ . Nucleotide binding to Ras is accompanied by a slow kinetic step that may correspond to a local folding event (72, 78). Both the  $\alpha$  and  $\beta$  phosphates are required to ensure tight binding; the affinity of Ras (72) for guanosine and GMP is six orders of magnitude lower than for GDP or GTP. Similar trends are observed for the  $G_{\alpha}$  subunits of heterotrimeric G proteins (81).

The GTP- and  $Mg^{2+}$ -binding sites are tightly coupled. In the absence of  $Mg^{2+}$ , the rate at which GTP dissociates from  $G_{i\alpha}$  and  $G_{o\alpha}$  increases at least 10-fold (79, 82); conversely, at a free  $Mg^{2+}$  concentration  $\leq 100$  nM, bound GTP $\gamma$ S is virtually nondissociable. The same effects of  $Mg^{2+}$  on GTP binding are also discussed for Ras (73, 83). In contrast, the degree to which  $Mg^{2+}$  is necessary to support GDP binding is not the same for all G proteins. Ras (83) and EF-Tu (84) form tight and nearly irreversible GDP  $\cdot$   $Mg^{2+}$  complexes;  $Mg^{2+}$  binds with micromolar affinity to the Ras  $\cdot$  GDP complex and reduces the GDP off-rate by four orders of magnitude (85). On the other hand, G proteins such as  $G_{i\alpha}$ ,  $G_{o\alpha}$ , and  $G_{s\alpha}$  [but not  $G_{t\alpha}$  (86)] bind GDP with lower affinity than they bind GTP; dissociation rate constants are on the order of  $10^{-2}$   $s^{-1}$ . Furthermore, the GDP complexes of these proteins have little affinity for  $Mg^{2+}$ ; and in turn,  $Mg^{2+}$  has no effect on GDP binding (79). All  $G_{\alpha}$  subunits do not display a (relatively) low GDP affinity.  $G_{z\alpha}$  is similar to Ras in its high,  $Mg^{2+}$ -dependent affinity for GDP (87).  $G_{q\alpha}$  and  $G_{11\alpha}$  also have some unique properties: Relatively high (30  $\mu$ M) concentrations of GTP $\gamma$ S are required for half maximal activity, yet GDP dissociation rates are unusually slow (88). For the most part, G proteins that incorporate  $Mg^{2+}$  into the GDP complex bind the nucleoside diphosphate more tightly than those that do not. Linkage between the GTP  $\gamma$ -phosphate site and the  $Mg^{2+}$  may depend on the rigidity of the switch I/switch II interface. As described below, the  $\gamma$ -phosphate of the nucleotide reinforces this linkage; thus, its loss upon hydrolysis may be more destabilizing in some G proteins than in others. Finally, the disposition of the conserved Asp residue in the G-3 region, which coordinates the  $Mg^{2+}$  through a water molecule in the second coordination sphere, may be critical. The overall structure of the protein—the presence or absence of a helical domain to buttress the nucleotide-binding site, for example—does not appear to be a critical factor. Even though the structures

of their nucleotide-binding sites are virtually identical, the GDP exchange rate is about a day for  $G_{i\alpha}$  (86) and on the order of minutes for  $G_{i\alpha 1}$ . It is difficult to provide a structural rationale for the observed differences among  $G_{\alpha}$  subunits in nucleotide (particularly GDP) affinity. Admittedly, however, these differences may be quite subtle since the observed differences in binding affinity represent free energies that differ by only 1–3 kcal/mol.

The residues that bind to the guanosine diphosphate moiety form a rigidly conserved structural unit common to all G proteins (Figure 2). The  $\alpha$ - and  $\beta$ -phosphates of the nucleotide are enfolded by the P-loop (G-1), which offers four backbone amides as the hydrogen-bond donors to the phosphate oxygen acceptors. The  $\alpha$ -phosphate of the nucleotide forms only one or two hydrogen bonds, which perhaps explains why GMP binds relatively weakly. The unusual and highly specialized conformation of the P-loop is facilitated by two conserved Gly residues (amino acids 10 and 15 in Ras) (Table 1) that adopt main-chain torsional angles that are sterically unfavorable for all residues but Gly. Nevertheless, the P-loop is rigid in both the crystal structures of G proteins and the solution structure of Ras (38) and does not participate in any of the conformational changes that occur upon GTP hydrolysis. Many of the mutations at Gly-12 that reduce the hydrolytic activity of Ras (23, 33) do not perturb the conformation of the P-loop itself (31, 33, 89). The K and (S or T) side chains of the P-loop are critical. The Lys residue bridges the  $\beta$ - and  $\gamma$ -phosphates; absence of this side chain in EF-G (49) may account for its comparatively low affinity for GTP and GDP (77). The hydroxyl of the Ser (or Thr) helps coordinate  $Mg^{2+}$  (see below).

The  $Mg^{2+}$ - and  $\gamma$ -phosphate-binding sites converge at the two most plastic regions of the G domain, G-2 (effector loop, switch I) and G-3 (switch II) (Figure 2). In GTP complexes,  $Mg^{2+}$  is hexacoordinate, and two of its ligands are supplied by the  $\beta$ - and  $\gamma$ -phosphates. Two more ligands are provided by the P-loop Ser (or Thr), which donates a hydroxyl group, as does the conserved Thr in G-2. Water molecules constitute the fifth and sixth ligands to the  $Mg^{2+}$ . One of these water molecules is coordinated by the conserved Asp in the G-3 motif and the other is hydrogen-bonded to an  $\alpha$ -phosphate oxygen atom. In EF-Tu, the second water molecule is hydrogen-bonded to an Asp in the extended effector loop region that follows helix  $\alpha 1$  but has no counterpart in the other G protein structures. The  $\gamma$ -phosphate of GTP forms hydrogen bonds to the main-chain amide of the conserved Gly in the DXXG sequence (G-3), near the N-terminal end of the switch II helix, and to the hydroxyl group and main-chain amide of the G-1 loop Ser (or Thr), which also helps coordinate the  $Mg^{2+}$ . In Ras, the hydroxyl group of Tyr-32 in the switch I region is also a  $\gamma$ -phosphate ligand. Mutation of the G-2 Ser in  $G_{o\alpha}$  (90) and  $G_{i\alpha 2}$  (91) abolishes GTP $\gamma$ S binding

yet does not disrupt interaction with the cognate  $\beta\gamma$  subunits, thereby creating a dominant-negative phenotype. The  $\text{Mg}^{2+}$  affinity of the corresponding S47N mutant in  $G_{i\alpha 1}$  is reduced by  $10^4$  (DM Berman & AG Gilman, unpublished data). A mutagenic scan of  $G_{o\alpha}$  generated many mutations that reduced affinity for  $\text{GTP}\gamma\text{S}$  but could be rescued to varying degrees by  $\text{Mg}^{2+}$  (90). Many of these mutations occurred in or near the G-1, G-2, or G-3 sequences, but others were rather distant from these regions. Indeed, truncation of the C-terminal 14 residues of  $G_{o\alpha}$  decreases affinity for GDP with little change in that for  $\text{GTP}\gamma\text{S}$  (92). Studies with  $G_{i\alpha 1}/G_{o\alpha}$  chimeras suggest that truncation abolishes a stable interface between the  $\beta 1$  and  $\beta 3$  strands and a three-residue hydrophobic surface on  $\alpha 5$  that contributes to GDP affinity (93). Specific mechanisms could be postulated to explain these effects; for example, localized perturbation of helix  $\alpha 5$  could destabilize G-5. It is also likely, however, that mutations that are more globally disruptive could alter ligand affinity. Since GDP is less tightly bound by  $G_{\alpha}$  subunits than GTP, effects of mutations would be more readily manifested as changes in GDP affinity.

Upon GTP hydrolysis, the  $\gamma$ -phosphate/ $\text{Mg}^{2+}$  scaffold is dismantled. In crystals of Ras (15) (Figure 1, *bottom*), ARF-1 (42), Ran (40a), and EF-Tu (18, 18a, 47b) (Figure 3, *bottom*) prepared with GDP and millimolar  $\text{Mg}^{2+}$ , the metal ion coordination sphere has lost the  $\gamma$ -phosphate anion and the Ser (or Thr) hydroxyl from the effector loop. These ligands are replaced by water molecules. The switch II helix collapses owing to loss of contact between the conserved Gly (of G-3) and the  $\gamma$ -phosphate; in  $G_{i\alpha 1}$  and  $G_{t\alpha}$ , the Asp in G-3 that polarizes a water ligand of the  $\text{Mg}^{2+}$  is also displaced. It is perhaps for this reason that these  $G_{\alpha}$  subunits have less affinity for  $\text{Mg}^{2+}$  in the GDP-bound state than Ras. ARF-1 also appears to have low affinity for  $\text{Mg}^{2+}$  in the GDP-bound state. In the structure of rat ARF-1 (42), only five ligands are directly coordinated to  $\text{Mg}^{2+}$ . All of these are water molecules, with the exception of the G-1 Thr hydroxyl group and an oxygen atom from the  $\beta$ -phosphate. Due to a two-residue shift (relative to Ras) in the position of the G-3 DXXG sequence, the conserved Asp is not a water-mediated  $\text{Mg}^{2+}$  ligand. In contrast, seven ligands are observed in the metal coordination sphere of human ARF-1 (41), although it is possible that the identity of the latter is  $\text{Ca}^{2+}$ , rather than  $\text{Mg}^{2+}$  (41).

As shown in Figure 2, the first and last residues of the NKXD (G-4) sequence specifically hydrogen bond to the guanine ring of the bound nucleotide. The methylene groups of the Lys side chain in the G-4 motif provides a hydrophobic surface that lies over the purine ring; and, in some structures, the  $\epsilon$ -amino group of the Lys side chain is hydrogen-bonded with an endocyclic oxygen atom of the ribose ring (e.g. in EF-Tu and Ras). In  $G_{i\alpha 1}$  and  $G_{t\alpha}$ , this Lys residue in G-4 forms an ion pair with Asp-150 in the loop preceding the

$\alpha$ E-helix in the helical domain. The exocyclic keto oxygen at position 6 of the guanine ring is hydrogen-bonded to a main-chain amide in G-5. Loss of this interaction, as would occur with binding of an inosine nucleotide, results in a reduction in affinity of two to three orders of magnitude (94). G proteins are selective for guanine nucleotides because they discriminate against adenine nucleotides; in the case of Ras (94) and EF-Tu (78), GTP binds better than ATP by seven orders of magnitude. The relative lack of affinity for adenine nucleotides is due not only to loss of a favorable interaction (with Asp-119) at the 1 position of the adenine ring, but also to the unfavorable juxtaposition of two hydrogen-bond donors, the exocyclic  $\text{NH}_2$  at position 6 of the adenine ring with the amido group of Asn-116. Mutation of Asp-119 in Ras (95) or Asp-138 in EF-Tu (96) neatly switches the specificity of the active site from guanine to xanthosine with the expected changes in activity in vivo (97, 98). G proteins show much variation in the way they stabilize the purine ring on the side opposite G-4. In Ras, support comes from Phe-28 near the G-2 box; but in other G proteins, residues in the  $\beta 6$ - $\alpha 5$  loop serve this function, e.g. Thr-327 in  $G_{i\alpha 1}$ . In most G protein complexes, the hydroxyl groups of the ribose ring of the guanine nucleotide form hydrogen bonds with main-chain carbonyl or side-chain carboxylate groups in residues near the G-2 region but are otherwise solvent accessible. Consequently, fluorescent probes, such as 2'(3')-O-(N-methylanthraniloyl) GTP (mant-GTP) (a fluorescent GTP analog) (72, 99), bind with affinities and are hydrolyzed at rates similar to GTP itself, indicating that modification of the ribose ring at these positions causes little perturbation of the three-dimensional structure of the protein (34). In  $G_{i\alpha 1}$ , the ribose projects toward the helical domain but makes no direct contact. Although the helical domain forms one wall of the GTP-binding site, it appears to provide little binding energy; in fact, the rate of dissociation of GDP from  $G_{i\alpha}$  and  $G_{s\alpha}$  is much higher than that from Ras, which possesses no helical domain (see below).

## STRUCTURAL CHANGES UPON GTP BINDING: EFFECTOR RECOGNITION

A G protein uses the binding energy of GTP to stabilize the switch regions to produce a conformation that permits its association with effector. This energy is dissipated upon GTP hydrolysis. For Ras and  $G_{\alpha}$  subunits, the overall structural consequences are not dramatic, except for the changes in the conformation and mobility of the effector-binding switch regions. In reciprocal fashion, the energy derived from the G protein-effector interaction contributes to the stability of the GTP complex and, in some cases, promotes approach to the transition state for GTP hydrolysis. In contrast to Ras, GTP hydrolysis in

EF-Tu triggers massive domain rearrangements; even so, interaction of EF-Tu with the ribosome is required to generate its catalytically competent state.

### *Ras-Effector Interactions*

In Ras, binding of GTP · Mg<sup>2+</sup> maintains the active conformation of the switch II and switch I regions as described above (Figure 1, *top*). GTP hydrolysis induces an ordered coil → helix transition at the N-terminus of switch II and subsequent reorientation of the entire  $\alpha 2$  helix (for review see 1a and 100), thereby dismantling the effector-binding site (Figure 1, *bottom*). However, even in the GTP-bound form, switch II is relatively mobile. Gly-60 in the switch II DXXG-motif is a critical pivot for the reorientation and partial refolding of the helical region of switch II (30) because its main-chain amide forms a hydrogen bond with the  $\gamma$ -phosphate. A Gly-60 Ala mutation inhibits the GTP-induced conformational change and reduces the affinity of Ras for its effector, Raf (101). The corresponding mutations in G<sub>Ser</sub> (80, 102), G<sub>I $\alpha$ 1</sub> (103), and EF-Tu (104) have analogous outcomes, confirming that this Gly residue plays a critical role in all G proteins.

The conformational transition in switch I is manifested in reorientation of both Tyr-32 and the conserved Mg<sup>2+</sup> ligand in the G-2 box, Thr-35, both of which are ligands to the  $\gamma$ -phosphate of GTP. Thus, the conformational changes in the two switch regions are coupled.

Mutagenic studies have implicated both switch regions of Ras in Ras-GAP and effector binding (37, 105). One of the effectors of Ras is Raf-1, a Ser/Thr-directed protein kinase that acts upstream of MEKK in the MAP kinase pathway (see 106 for review). Raf-1 contains an 80-residue domain (RBD, for Ras-binding domain) that can be expressed independently and is sufficient for GTP-dependent binding of Ras. The crystal structure of RBD complexed with the GppNp · Mg<sup>2+</sup> form of Rap1A has recently been determined (39). Rap1A is a catalytically inactive (Q61T) cytosolic homolog of Ras that inhibits the Ras-dependent activation of MAP kinase (107). The primary structures of Rap1A and Ras are identical within the effector loop residues (32–40). As predicted from mutagenesis studies of Ras (37), the effector loop, in addition to the following  $\beta 2$ - $\beta 3$  strands of Rap1A, forms the entirety of the site recognized by the RAF-1 RBD. The RBD consists of a tertiary fold that is the structural analog of ubiquitin (108) and interacts with Rap1, in part, through an antiparallel  $\beta$ - $\beta$  contact, involving the B2  $\beta$  strand of RBD and  $\beta 2$  in Rap1, together with a single Arg side chain at the C-terminal end of the A1 helix of the RBD (39). Differences in Rap1A/RBD association energy resulting from mutations of residues in the G-2 region (switch I) of Rap1 are quantitatively correlated with the extent to which the same mutations in Ras permit residual activation of MAP kinase *in vivo* (109). The switch II region of Rap1A, and residues that

directly form the GTP recognition site, do not participate in the interaction with the RBD of Raf-1. Yet switch II is indirectly involved in recognition because its conformational change is coupled to that of the switch I effector-binding loop, as described above (see also 109a, 109b). It may be significant that the switch II element remains exposed in the RBD-Rap1A complex because it is the site of many of the mutations that disrupt Ras binding to Ras-GAP (37). Consequently, Ras-GAP might be able to bind to the Raf-1 · Ras · GTP · Mg<sup>2+</sup> complex directly and thereby induce hydrolysis of GTP and the subsequent release of Raf-1. Indeed, a model for Ras · Ras-GAP interaction based on the crystal structure of the catalytic domain of p120<sup>Ras-GAP</sup> (109c) proposes a significant role for the switch II region of Ras in binding to Ras-GAP. Although much of the mutational data on Ras can be rationalized by the RBD · Rap1A structure, the locations of intragenic suppression mutations in Raf-1 indicate that portions of the protein kinase outside of the RBD domain are involved in the interaction of native Raf-1 with Ras · GTP · Mg<sup>2+</sup>.

### *The Complex of Elongation Factor Tu with Amino-Acyl tRNA*

Binding of GTP to EF-Tu triggers a conformational change in switch II that is roughly similar to that in Ras, but the consequences to the global structure of EF-Tu are far more dramatic (Figure 3, *top*). In this case, the peptide group of Gly-84 in switch II flips 180°, allowing its amide group to form a hydrogen bond to the  $\gamma$ -phosphate of GTP. This induces the amino terminus of the switch II helix to unwind and the entire helix to reorient, thereby creating a binding site for domains 2 and 3. Together, these two domains rotate as a rigid unit by 90°, leaving domain 3 packed against the switch II helix (Figure 3, *top*). The interface between these domains is populated by polar and charged residues, as expected for a dynamic contact surface (17). This movement closes the cavity between the three domains that is present in the GDP form of the molecule (Figure 3, *bottom*), and creates a negatively charged cleft between the G domain and domain 2 that forms the binding site for the acceptor stem and 5'-end of the AA-tRNA. Also in the GppNp · Mg<sup>2+</sup> complex of the *T. thermophilus* (17) and *T. aquaticus* (19) factors, the effector loop is transformed from a  $\beta$ -hairpin into an extended strand preceded by two short perpendicular helices. This transition juxtaposes the conserved G-2 Thr with the Mg<sup>2+</sup> and thereby contributes to GppNp and Mg<sup>2+</sup> binding. The ordered effector loop forms a part of the cleft that receives the CCA (3') stem of AA-tRNA along with a surface of domain 2 (50). The aminoacylated 5'-terminus of the tRNA binds at an interface formed by all three domains, with a registration that prevents high-affinity association of nonacylated tRNAs. The T-stem of the tRNA interacts with the third domain. Still exposed in the EF-Tu · AA-tRNA complex is a conserved region of the effector loop that constitutes part of the ribosomal

binding site (47). Overall, there is little difference in structure between free EF-Tu · GppNp · Mg<sup>2+</sup> and that bound to AA-tRNA. Presumably, therefore, it is those conformational changes effected by interaction of the binary complex with the ribosome that stimulate GTP hydrolysis.

### *Effector Interactions with G<sub>α</sub> Subunits*

Unlike Ras and EF-Tu, no crystal structure has yet been determined for the complex between the α subunit of a heterotrimeric G protein and its effector. Nevertheless, chimeric proteins created from α subunits that interact specifically with different effectors have identified potential effector-binding sites. In addition, structures of G<sub>iα1</sub> and G<sub>tα</sub> in the GTPγS · Mg<sup>2+</sup> (Figure 4, *top*) and GDP-bound states (Figure 4, *bottom*) show how the candidate effector-binding regions are affected by GTP binding and hydrolysis. After an extensive analysis of G<sub>iα2</sub>/G<sub>sα</sub> chimeras, Berlot & Bourne (110) identified three regions within the G domain of G<sub>sα</sub> that are required for adenylyl cyclase activation. The first corresponds to the C terminus of the α2 helix, a segment that is encompassed by switch II (Figure 3). A second region, also identified by Itoh & Gilman (111), maps to the loop connecting helix α3 to strand β5. The third region corresponds to the loop that connects helix α4 to strand β6. A peptide corresponding to the latter region in G<sub>α</sub> was also found to activate cGMP phosphodiesterase (PDE) (112) through its interaction with the C terminus of the γ subunit of PDE (see 54 for a review). In G<sub>tα</sub>, switch II (113) and the α3 helix with the following α3-β5 loop are also implicated in GTPγS · Mg<sup>2+</sup>-dependent binding of PDEγ (114). Thus, it appears that roughly the same surfaces of G<sub>sα</sub> and G<sub>tα</sub>—all located on the same face of each subunit—are involved in effector recognition, even though there is nothing to suggest that the effectors themselves are structurally similar. Recently, Hepler et al (115) demonstrated that Cys-9 and Cys-10 of G<sub>qα</sub>, whether palmitoylated or not, are required for activation of phospholipase C-β1, indicating that the N terminus of a G<sub>α</sub> subunit may contribute to recognition of its effector.

Three segments of G<sub>iα1</sub> (22) and G<sub>tα</sub> (20) undergo substantial rearrangement upon GTP hydrolysis. These are switch I (the “effector” loop), switch II (the loop preceding the α2 helix, and the helix itself), and switch III, which comprises the loop connecting helix α3 to strand β5. The latter two correspond to proposed effector-binding regions. The nature of the conformational change in G<sub>iα1</sub> is somewhat different from that in G<sub>tα</sub>, but the three switch regions undergo rearrangements that are coupled in approximately the same way. When both molecules are in the GTPγS · Mg<sup>2+</sup>-bound state (Figure 4, *top*), basic residues in helix α2 form ionic interactions with complementary residues in the switch III loop. Collapse of the ordered switch II helix upon GTP hydrolysis, similar to what is seen in Ras, severs these contacts. Associated with these changes is a

small rotation that opens the cleft between the G domain and the helical domain, slightly increasing accessibility of the GDP-binding site. In  $G_{i\alpha 1}$ , the switch II and III regions simply become disordered (Figure 4, *bottom*); in  $G_{i\alpha}$ , they adopt different conformations but are no longer in contact. These structural changes are perhaps sufficient to account for the observed 70-fold difference in affinity for PDE $\gamma$  between the GTP- and GDP-bound states of  $G_{i\alpha}$  (114) and for the 10-fold difference in affinity for adenylyl cyclase between the two states of  $G_{s\alpha}$  (56). These rather modest changes in effector affinity suggest that the switch regions are relatively plastic and that the primary activating effect of GTP is assisting in their organization. Thus, the driving force for GTP hydrolysis is mainly entropic. Remarkably, mutation of Glu-203 in switch II of  $G_{i\alpha}$  (equivalent to position 207 in  $G_{i\alpha 1}$ ) to Ala allows the mutant protein in the GDP-bound state to activate PDE $\gamma$  (116). The structural basis for this effect is not obvious because upon GTP binding the mutant exhibits the expected enhancement in fluorescence of Trp-207 (also in switch II) (see below) that is characteristic of the wild-type subunit upon GTP binding. Possibly the Glu-203 Ala mutation alters flexibility of switch II rather than the landscape of the effector-binding site in  $G_{i\alpha}$ . The three-dimensional structures of  $G_{i\alpha 1}$  and  $G_{i\alpha}$  also explain two phenomena that have long been associated with the transition from the GTP- to the GDP-bound state: (a) a decrease in amplitude of the intrinsic fluorescence (82, 117) of Trp-207 (in  $G_{i\alpha}$ ) (113); and (b) an increased susceptibility to degradation by trypsin (102, 118, 119). Both effects clearly arise from the movement of affected residues from a buried environment to the solvent-exposed milieu.

An unexpected synergy between the switch II and switch III regions and the N- and C-termini  $G_{i\alpha 1}$  is revealed by comparing the GDP (22) and GTP $\gamma$ S · Mg<sup>2+</sup>-bound (21) conformations. Whereas both switches II and III are well ordered in the GTP-bound state, the N-terminal 32 and C-terminal 10 residues are disordered (Figure 4, *top*). In the GDP-bound state, the switch II and III regions are disordered, but residues 8–32 and 344–354 fold into a compact microdomain. A sulfate ion derived from the crystallization medium—perhaps mimicking a phosphate ion—helps to organize this domain through interactions with a triad of conserved basic residues (Figure 4, *bottom*). This refolding and association of the N and C termini may explain the insensitivity of free  $G_{i\alpha}$  subunits to pertussis toxin-mediated ADP ribosylation (11). The N terminus of other G proteins may also be a flexible structure that can adopt a stable structure if offered a suitably complementary surface on which to fold (see below). In this regard, N-terminal order/disorder transitions, analogous to those in  $G_{i\alpha 1}$ , may be involved in the transfer of ARF from its membrane-bound condition in the GTP-bound state to its cytosolic location in the GDP-bound state. The  $G_{i\alpha 1}$  · GDP structure holds yet more surprises in the form of

quaternary contacts between the terminal microdomain of one molecule and a horseshoe-shaped cavity formed by the helical domain of a second, symmetry-related molecule. The switch I strand forms part of the contact surface, so in the crystal, formation of polymers is linked to conformational changes of the switch elements. The surface area involved in this contact is comparable to that observed in antibody-antigen interactions. A conformational change in the loop connecting  $\alpha B$  and  $\alpha C$  in the helical domain (switch IV) facilitates the  $G_{i\alpha 1}$ - $G_{i\alpha 1}$  contacts. There is some evidence that such quaternary interactions may occur *in vivo*. Nakamura & Rodbell have reported the presence of G protein aggregates in hepatocyte membranes that disappear upon activation of glucagon-responsive receptors (120). Other accounts of  $G_{\alpha}$ - $G_{\alpha}$  cross-links have been published (121); perhaps the most intriguing is the demonstration that a 2-azido-ADP-ribosyl group that can be photoactivated can be transferred from Cys-347 of one  $G_{i\alpha}$  subunit to the amino terminus of a second (122). A variety of roles for  $G_{\alpha}$  polymerization/aggregation have been proposed, including aggregation/disaggregation mechanisms for G protein-dependent signaling (123),  $G_{\beta\gamma}$ - or receptor-independent mechanisms of nucleotide exchange (22), and propinquity-priming of  $G_{\alpha}$  subunits for efficient (serial) coupling to receptors (124). Perhaps the real significance of  $G_{\alpha}$  homopolymers, if indeed there is any, will be found in the context of complexes with cytoskeletal components, such as actin or tubulin, or with membrane compartments (reviewed in 125), such as caveoli (126).

## MECHANISM OF GTP HYDROLYSIS

Some G proteins, such as  $G_{i\alpha 1}$ , are sluggish GTP hydrolases [turnover number of  $3 \text{ min}^{-1}$  (11)]; others, such as Ras ( $0.03 \text{ min}^{-1}$ ) (127) and EF-Tu ( $0.003 \text{ min}^{-1}$ ) (128), are marginally catalytic. Isotopic labeling shows that, in EF-G (129), EF-Tu (130), and Ras (131), GTP is hydrolyzed via an  $S_N2$  mechanism—direct in-line transfer of the  $\gamma$ -phosphate from GTP to water, with inversion of configuration around the phosphate. Attempts have been made to identify a residue that could serve as a catalytic base to activate water for nucleophilic attack. For some time, attention was focused on a Gln residue (position 61 in Ras). This side chain resides in the G-3 box (Table 1) and, with a few exceptions (like EF-G, EF-Tu, and Rap1A) is conserved in most members of the G protein family. Virtually all mutations at this site in Ras reduce its GTPase activity 10-fold, prevent response to Ras-GAP, and are oncogenic (132, 133). Corresponding mutations (at Gln-227) in  $G_{s\alpha}$  (60, 134, 135) and (at Gln-204) in  $G_{i\alpha 1}$  (21) also abolish GTPase activity. In complexes of Ras,  $G_{i\alpha}$ , and  $G_{i\alpha 1}$  with nonhydrolyzable GTP analogs, the equivalent Gln is within hydrogen-bonding distance of the water molecule that is the presumptive nucleophile. This water

molecule is situated less than 4.0 Å from the  $\gamma$ -phosphorus, positioned for in-line attack, and stabilized by hydrogen bonding both to an oxygen of the  $\gamma$ -phosphate and to the conserved Thr in the G-2 loop. Several of the mutations of Gly-12 in the P-loop of Ras, which reduce GTPase activity and are oncogenic, perturb the conformation of Gln-61 or its interaction with the presumed water nucleophile (33, 89).

The structure of Ras · GppNp · Mg<sup>2+</sup> (14), and the observation that a Q61E mutation increases the turnover number for GTP hydrolysis (136), supports the view that water is activated for nucleophilic attack on the  $\gamma$ -phosphate by Gln-61 and the backbone carbonyl of Thr-35. However, Privé et al (31) noted that mutations at position 61 do not alter the position of the bound water molecule and that Gln (with a pK<sub>b</sub> of ~15, compared to a pK<sub>b</sub> for ammonia of ~5) is too weak a base to abstract a proton. Free-energy perturbation calculations (137) also indicate that Gln-61 is unlikely to serve as a general base. Perhaps most telling is the demonstration that substitution at residue 61 in Ras of a nitroglutamate, an unnatural amino acid that is isoelectronic and isosteric to Gln, has no effect on the GTPase activity of Ras (138). Nitroglutamate is expected to be an even poorer hydrogen acceptor than Gln (with a pK<sub>b</sub> of greater than 17). Privé et al proposed an alternative role for Gln-61, namely, direct stabilization of the pentavalent transition state (31). This proposal is supported by the structures of both G<sub>iα1</sub> and G<sub>1α</sub> complexed to GDP and aluminum fluoride, as described below. A better candidate than Gln-61 for the general base in Ras has not emerged [the nearby Glu-63, and its cognate Glu-207 in G<sub>iα1</sub>, have been ruled out by mutagenesis (139)]. Valence bond calculations indicate that catalysis could be substrate-assisted, with the  $\gamma$ -phosphate of GTP serving as the base (140). In Ras, pH-activity profiles provide evidence for involvement in the reaction mechanism of a group with a pK<sub>a</sub> near 3; a sharp transition in the chemical shift of an enzyme-bound <sup>31</sup>P implicated the  $\gamma$ -phosphate of GTP as that group (141).

Aluminum fluoride is a strong activator of G<sub>α</sub> subunits (142) and binds with GDP to the active site as a tetracoordinate AlF<sub>4</sub><sup>-</sup> (142, 143) or AlF<sub>3</sub>(OH)<sup>-</sup> (144, 145) ion. It was proposed initially that aluminum fluoride mimics the  $\gamma$ -phosphate of GTP. It is now clear that the bound AlF<sub>4</sub><sup>-</sup> mimics the  $\gamma$ -phosphate in its pentavalent transition state during hydrolysis. In the G<sub>iα1</sub> · GDP · AlF<sub>4</sub><sup>-</sup> · Mg<sup>2+</sup> (at 2.3 Å resolution) (21) and G<sub>1α</sub> · GDP · AlF<sub>4</sub><sup>-</sup> · Ca<sup>2+</sup> (at 1.7 Å) (146) structures (Figure 5), the fluoroaluminate appears in a square planar configuration, with an oxygen of the GDP  $\beta$  phosphate and a water molecule serving as the transaxial ligands to complete a tetragonal bipyramid. In this complex, the carboxamido moiety of Gln-204 (in G<sub>iα1</sub>) is hydrogen-bonded to the transaxial water molecule, possibly as an acceptor, and to one of the periplanar fluorides, as a donor. In this arrangement, Gln-204 is proposed to

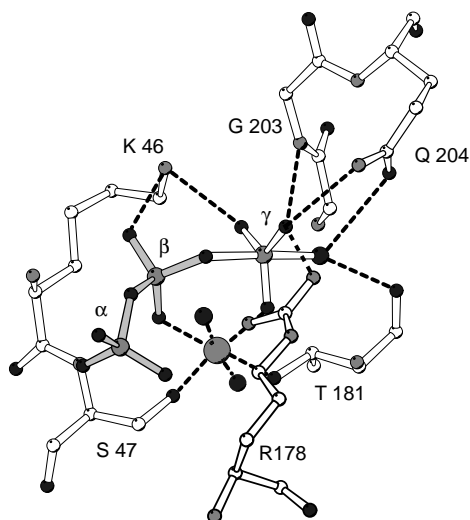


*Figure 5* A model of the transition state for  $G_{i\alpha 1}$ -catalyzed GTP hydrolysis (derived from the crystal structure of the  $GDP \cdot AlF^- \cdot Mg^{2+}$  complex, PDB entry 1GFI). Residues are identified by the one-letter code; carbon, nitrogen, and oxygen atoms are depicted as white, gray, and black small spheres, respectively; water molecules are depicted as larger black spheres (as is the axial ligand of the pentacoordinate  $\gamma$ -phosphate), phosphorus as larger gray spheres, and  $Mg^{2+}$  as a large gray sphere. P-O bonds of the  $\alpha$ - and  $\beta$ -phosphate groups are darkened. Hydrogen bonds, and coordination contacts with the  $Mg^{2+}$  are depicted with dashed lines.

polarize and orient the nucleophilic water molecule in the transition state for hydrolysis (21). A similar configuration is observed in  $G_{t\alpha}$ , but two alternative mechanisms have been proposed to explain how Gln assists in the abstraction of a proton from the nucleophile by the leaving group (137, 140). In one of these mechanisms, involvement of the imino tautomer of Gln is postulated (146). Arg-178 (in G-2) of  $G_{i\alpha 1}$  (174 in  $G_{t\alpha}$ ) coordinates a second fluoride and the  $\beta$ -phosphate oxygen that forms a ligand to the fluoroaluminat. In the transition state, Arg-178 is proposed to stabilize the developing negative charge on the pentavalent phosphate leaving group, thereby facilitating its release (19, 21). It is for this reason that cholera toxin-catalyzed ADP ribosylation of Arg-174 in  $G_{t\alpha}$  (71) [or the equivalent Arg-201 in  $G_{s\alpha}$  (59)] abolishes GTPase activity (147), as do mutations of these same residues (21, 60). In  $G_{i\alpha 1}$ , Gln-204 and Arg-178 do not stabilize the ground state  $GTP\gamma S \cdot Mg^{2+}$  complex: Both are partially disordered in the  $G_{i\alpha 1} \cdot GTP\gamma S \cdot Mg^{2+}$  complex [although Arg-174 is an ordered ligand of the  $\beta$ - and  $\gamma$ -phosphates in the corresponding  $G_{t\alpha}$  structure (19)]. Further, in  $G_{i\alpha 1}$ , the Q204L and R178C mutants bind  $GTP\gamma S \cdot Mg^{2+}$

normally (21), as does a Q61L mutant of Ras (31). In contrast, both mutations selectively reduce the affinity of  $G_{i\alpha 1}$  for  $GDP \cdot AlF_4^- \cdot Mg^{2+}$  (21). Neither of the proposed catalytic Arg and Gln residues just discussed is completely conserved in the G protein superfamily.

Unlike  $G_\alpha$  subunits, neither  $Ras \cdot GDP \cdot Mg^{2+}$  (148) nor  $EF-Tu \cdot GDP \cdot Mg^{2+}$  (149) binds aluminum fluoride. To the extent that aluminum fluoride is mimetic of the metastable bipyramidal transition state intermediate, it can not contribute enough binding energy to stabilize a transition state-like conformation of these less active GTP hydrolases. It has been suggested that the helical domain of a  $G_\alpha$  subunit provides the additional stabilization energy not available to Ras and EF-Tu. Markby et al (57) have shown that an independently folded fragment of  $G_{s\alpha}$  that corresponds to the helical domain (and contains Arg-201) is capable of stimulating the GTPase activity of the remaining G domain fragment. In  $G_{s\alpha}$ , mutation of Lys-278 (in G-4) and Asp-158, for which the corresponding residues also participate in an interdomain ion pair in  $G_{i\alpha 1}$  and  $G_{i\alpha}$ , abolishes activation by  $GDP \cdot Mg^{2+} \cdot AlF_4^-$  binding, but not  $GTP\gamma S \cdot Mg^{2+}$ -simulated cyclase activation (150). On the other hand,  $G_{z\alpha}$ , in which both a Arg-174 (Table 1) and a helical domain are present, is no better a GTPase than Ras (87). However, the relatively weak hydrolytic activity of  $G_{z\alpha}$  may arise from the substitution of the second Gly by a Ser in the conserved (in  $G_\alpha$  subunits) G-1 box GAGES sequence (A Raw & Gilman, unpublished results.)

The structures of the  $GTP\gamma S \cdot Mg^{2+}$  and  $GDP \cdot AlF_4^- \cdot Mg^{2+}$  complexes of  $G_{i\alpha 1}$  and  $G_{i\alpha}$  provide strong evidence that at least two side chains must be reoriented in the catalytic site during the course of catalysis. Decay of fluorescence emission of mant-GTP in Ras with a rate constant similar to that of GTP hydrolysis suggests that conformational changes in the switch regions are concomitant with bond cleavage or release of inorganic phosphate. The fluorescent group of mant-GTP interacts with Tyr-32 of G-2 (34), which undergoes a substantial conformation change upon GTP hydrolysis. Given the slow turnover rates of G proteins, it is reasonable to expect that conformational rearrangements of the catalytic Gln and Arg residues could correspond to the rate-limiting step. Attempts have been made to visualize intermediates in this process using Laue diffraction measurements of Ras crystals containing a caged GTP that can be activated by flash photolysis (32). More than one conformational transition may occur along the reaction trajectory for GTP hydrolysis. The recent discovery, in the crystal structure of the G203A mutant (in G-3) of  $G_{i\alpha 1}$ , of a conformational change in the switch II helix upon  $GDP \cdot Pi$  binding (103), suggests that conformational changes may attend the breakdown of the bipyramidal intermediate. All of the above structural rearrangements inferred from crystallographic studies of  $G_\alpha$  complexes would be subsumed within the events assayed by the single turnover rate of GTP hydrolysis.

The catalytic mechanism of GTP hydrolysis by EF-Tu may be quite different from that of the other G proteins discussed. In place of Ras Gln-61, EF-Tu possesses a His that is essential for GTP hydrolysis (152). In the GppNp complex of Ef-Tu (16, 17), His-85 in G-3 and the presumptive water nucleophile, together with Asp-86, are arrayed in a configuration reminiscent of the catalytic triad in serine proteases. Even in the GTP-activated state, His-85 would have to rotate in order to abstract a proton from the nucleophilic water. Rotation is blocked by a hydrophobic gate (17) between the G-1 and G-2 segments. Presumably, productive interaction of the EF-Tu · GTP · Mg<sup>2+</sup> · AA-tRNA complex with the ribosome is required to induce a conformational change that opens the gate.

Fundamental questions remain about the mechanism of GTP hydrolysis. Most have assumed that the transition state is associative, in which there is a considerable degree of bond formation between the  $\gamma$ -phosphate and the water nucleophile. Mechanistic studies of nonenzymic model reactions have led Maegley et al (153) to propose that the GTP hydrolysis reaction proceeds through a dissociative metaphosphate-like transition state, in which bond cleavage of the leaving group is nearly complete and bond formation with the nucleophile has barely occurred. This kind of transition state is characterized by a loss of negative charge on the phosphoryl group rather than by an accumulation as would occur in an associative mechanism. In a dissociative mechanism, a G protein would gain little advantage by trying to stabilize a developing negative charge on the incipient bipyramidal phosphate atom or by protonating this leaving group in the transition state. Other catalytic strategies are required (see 153 for review). The crystal structure of the GDP · Mg<sup>2+</sup> · AlF<sub>4</sub><sup>-</sup> complexes do not provide compelling evidence for one mechanism over the other because the G proteins seem poised to provide charge stabilization at both the bond-breaking and bond-forming steps.

## MECHANISM OF CATALYTIC RATE ENHANCEMENT BY GAP

The best-characterized GAPs are those that act upon Ras and its homologs (154). The p120<sup>Ras-GAP</sup> and neurofibromin (NF-1) proteins accelerate the rate of Ras-catalyzed GTP hydrolysis by four to five orders of magnitude (155, 156). Mutational analysis of Ras (see 37 for review) indicates that the switch I and switch II regions of Ras interact with Ras-GAPs. Because AlF<sub>4</sub><sup>-</sup> binds tightly to the Ras · GDP · Mg<sup>2+</sup> · GAP complex (157), whereas it fails to bind or activate Ras · GDP · Mg<sup>2+</sup> itself, Ras-GAP probably stabilizes Ras in a conformation that is most complementary to the pentacoordinate transition state of the  $\gamma$ -phosphate during GTP hydrolysis. GAPs could achieve this function by

providing a catalytic residue that Ras itself lacks, corresponding, for example, to the Arg-201 presented by the helical domain in  $G_{s\alpha}$  (57). Indeed, mutation of a single conserved Arg residue in NF-1 (157, 158) is sufficient to abolish its Ras-GAP activity. The three-dimensional structure of the catalytically active, 334-residue domain of the Ras-specific p120<sup>Ras-GAP</sup> (GAP-334) has recently been determined (109a). The protein fold comprises two  $\alpha$ -helical bundle domains. The larger, C-terminal domain contains, in a shallow groove formed by two helices, many of the residues that are most highly conserved among the different Ras-specific GAPs. From this structural data, a model was constructed in which the G-2 and the switch I and II regions of Ras are docked into a complementary site within the shallow groove of GAP-334. In this model, GAP-334 supplies two conserved Arg residues (789 and 903), one or both of which are proposed to stabilize the transition state for GTP hydrolysis.

The breakpoint-cluster-region homology (BcrH) of the phosphoinositide 3-kinase (PI3K) p85 $\alpha$  subunit possesses a three-dimensional fold that is superficially similar to that of the C-terminal domain of GAP-334 (158a), although no similarity in primary structure is evident. The BcrH domain of PI3K belongs to the family of RhoGAP domains found in proteins with GAP activity for members of the Rho class of small G proteins (158b). While the BcrH domain has not been demonstrated to possess GAP activity, it too presents a conserved residue in a shallow interhelical pocket that is proposed to constitute a potential Rho binding site (158a).

For certain  $G_\alpha$  subunits, notably  $G_{q\alpha}$  and  $G_{1\alpha}$ , the cognate effectors, phospholipase  $\beta$ 1 (159, 160) and the  $\gamma$  subunit of PGE (161), respectively, act as GAPs (see 162 for review). Rate enhancements are approximately 100-fold. Recently, a family of proteins that negatively regulate other  $G_\alpha$  subunits has been recognized. Collectively called RGS proteins (regulators of G protein signaling) (163), the first discovered was a protein (Sst2) that promotes  $G_\alpha$  inhibition of a yeast pheromone-mediated pathway that signals through  $\beta\gamma$  (164). The RGS family now comprises at least 15 mammalian gene products, including several detected by polymerase chain reaction amplification of rat brain cDNA (165). All members of the family are characterized by a  $\sim$ 130-residue RGS core domain that, in turn, is divided into three well-conserved segments (166). It is now clear that RGS proteins are GAPs (167–169) that selectively and potently (at least 50-fold acceleration of GTPase activity) activate members of the  $G_{i\alpha}$  and  $G_{o\alpha}$  classes. RGS4 acts catalytically, with a  $K_m$  for the interaction with  $G_{o\alpha} \cdot \text{GTP}$  of 2.5  $\mu\text{M}$  (170), and binds most tightly to the  $\text{GDP} \cdot \text{AlF}_4^-$  (168, 170) complex, with an apparent  $K_d$  below 100 nM, suggesting direct stabilization of the transition state conformation of  $G_\alpha$ . The Q204L mutant of  $G_{i\alpha 1}$  is not activated by RGS4, but the R178C mutant is stimulated weakly (167), paralleling the affinity of  $\text{GDP} \cdot \text{Mg}^{2+} \cdot \text{AlF}_4^-$  for the same  $G_{i\alpha 1}$

mutants (21). It is possible that RGS actually increases the affinity of the  $G_{i\alpha 1} \cdot \text{GTP}$  complex for  $\text{Mg}^{2+}$ , since maximal stimulation is observed even in the presence of 5 mM EDTA (167). The alternative possibility, that the catalytic mechanism becomes  $\text{Mg}^{2+}$  independent, is less likely, since RGS4 stimulation of the S47N mutant is highly  $\text{Mg}^{2+}$  dependent. The complex between RGS4 and  $\text{GDP} \cdot \text{AlF}_4^-$ -bound  $G_{i\alpha 1}$  has been crystallized (J Tesmer, DM Berman, AG Gilman & SR Sprang, unpublished results). A preliminary analysis shows that the RGS domain is comprised exclusively of  $\alpha$ -helices and contacts all three switch regions of  $G_{i\alpha 1}$ , locking the structure into a conformation similar to that observed in the  $G_{i\alpha 1} \cdot \text{Mg}^{2+} \cdot \text{GDP} \cdot \text{AlF}_4^-$  complex. Thus, to a first approximation, at least this  $G_\alpha$ -GAP stabilizes the conformation of the  $G_\alpha$  that recognizes the transition state.

## REGULATION OF GUANINE NUCLEOTIDE EXCHANGE

Although GDP dissociates slowly from isolated  $G_\alpha$  subunits, it binds almost irreversibly to  $G_{\alpha\beta\gamma}$  heterotrimers (11). Therefore,  $\beta\gamma$  dimers may be regarded as GDIs. However,  $\beta\gamma$  subunits can themselves play active roles in signal transduction (170a, 171), for example, through regulation of  $\text{K}^+$  channels, phospholipase  $C\beta$ , and certain isoforms of adenylyl cyclase in animal cells, and activation of the pheromone response pathway in budding yeast (171, 172). In this context, it is perhaps more accurate to characterize  $G_\alpha \cdot \text{GDP}$  as a  $\beta\gamma$  inhibitor. Thus,  $G_\alpha$ -catalyzed GTP hydrolysis serves a dual function by shutting off both  $\beta\gamma$ - and  $G_\alpha$ -mediated signaling pathways. The mechanism by which  $\beta\gamma$  subunits inhibit GDP release from  $G_\alpha$ , thereby rendering reactivation dependent upon  $G_\alpha$  interaction with ligand-activated membrane receptors, is an interesting example of active site remodeling as discussed below.

### *$\beta\gamma$ Subunits of Heterotrimeric G Proteins*

Five isoforms of  $\beta$  (173) and ten of  $\gamma$  (174) have been identified to date. The  $\beta$  isoforms share 50–90% identity in primary structure (172), but the sequences of  $\gamma$  subunits are more diverse (30–80% identity) (174). Mammalian  $\gamma$  subunits are modified at their C-terminus by the 20-carbon geranylgeranyl moiety or, in the case of  $\gamma_1$  and  $\gamma_{11}$ , the 15-carbon farnesyl moiety (174).  $\beta\gamma$  dimers are thus tethered to the plasma membrane (175). Nonprenylated  $\gamma$  dimerizes with  $\beta$  and the resulting dimers are soluble (176). However, prenylation of  $\gamma$  is required for high-affinity interactions of  $\beta\gamma$  with  $G_\alpha$  and adenylyl cyclase (177).  $\beta$  subunits depend upon  $\gamma$  to fold correctly (178–180); the two subunits cannot be dissociated from each other, except under denaturing conditions (181). Indeed, a significant conformational change appears to accompany  $\beta\gamma$  association because the Stokes radius of  $\beta$  decreases from 42 Å to 39 Å (181).

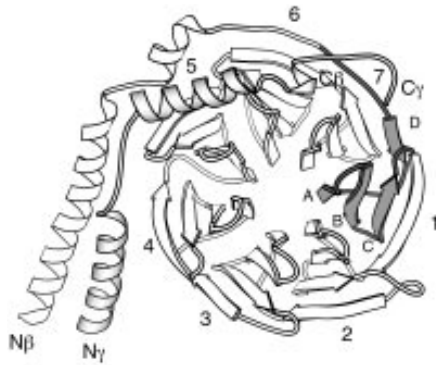


*Figure 6* Heterotrimeric G protein  $\beta_1\gamma_2$  heterodimer (extracted from PDB entry 1GG2). Structural elements corresponding to the first WD repeat are darkened and labeled. Each beta propeller is numbered, and the  $\gamma_2$  subunit is shaded.

$\beta$  and  $\gamma$  isoforms interact selectively. The  $G_T$ -associated  $\gamma$  subunit,  $\gamma_1$ , which is expressed exclusively in retinal rod cells, forms a complex with  $\beta_1$  but not  $\beta_2$  (even though  $\beta_2$  shares 93% sequence identity with  $\beta_1$ ) (177, 181, 182);  $\beta_2$  associates with  $\gamma_2$  but not  $\gamma_1$  (38% sequence identity to  $\gamma_2$ ) (181, 182). Except for  $\beta_1\gamma_1$ , which is expressed only in the retina, several combinations of  $\beta$  and  $\gamma$  subunits can interact with a single  $G_\alpha$  (183) and have similar activities, for example, in regulation of adenylyl cyclase isoforms (177), phospholipase *C $\beta$*  (184), or  $K^+$  channels (185).

Three-dimensional structures of  $\beta_1\gamma_2$  (186) and  $\beta_1\gamma_1$  (187) heterodimers reveal that the ( $\sim 80$ -residue)  $\gamma$  subunit is highly extended and embedded on one surface of the toroidal  $\beta$ -subunit (Figure 6). The major, 300-residue C-terminal domain of the  $\beta$  subunit adopts the so-called  $\beta$ -propeller fold, a motif that has been observed in a variety of other proteins (187a), many of which are unrelated to members of the  $G_\beta$  family. The  $\beta$ -propeller domain of the  $\beta$  subunit is composed of seven repeats of an  $\sim 43$ -residue sequence (188, 189), termed a WD repeat, that also occurs in a variety of functionally diverse proteins (190), although not in  $\beta$ -propeller domains generally. The  $\beta$ -propeller domain of  $G_\beta$  is formed by a series of seven four-stranded antiparallel  $\beta$  sheets, arranged like the blades of a propeller. Each WD repeat gives rise to four antiparallel strands, in part as previously predicted (190). However, a single WD repeat does not directly correspond to a single blade; rather, the most variable segment of each WD repeat, corresponding to its N-terminal portion ( $X_{8-15}$ , see below), forms the outermost, C-terminal strand of one blade, whereas the conserved core of the same repeat forms the three innermost strands of the next

blade. Therefore, a single WD repeat might not form a stably folded structure. The overall propeller structure of  $\beta$  is closed by juxtaposition of strands from the first and seventh WD repeats (Figure 4). When the structures of all seven blades are superimposed, a more detailed consensus emerges;  $X_{8-15}$ -[GHX<sub>3-5</sub> $\Phi$ X<sub>2</sub> $\Phi$ X $\Phi$ X<sub>5-6</sub> $\Phi$ <sub>2</sub>(S/T)(G/A)X<sub>3</sub>D X<sub>4</sub>WD], where X is any residue,  $\Phi$  denotes a hydrophobic residue, and parentheses enclose alternate possibilities (186, 187). Conserved hydrophobic residues contribute to the hydrophobic packing interactions between blades. The amino-proximal Asp is the only invariant residue in the motif; it stabilizes a five-residue loop between the second and third strands of each blade and participates in a hydrogen-bonded tetrad with the His, Ser (or Thr), and Trp residues where conserved.

The  $\gamma$  subunit in the  $\beta\gamma$  dimer is composed of two helical segments joined by a loop and has essentially no tertiary structure. The N-terminal helix of  $\gamma$  engages the N-terminal helix of  $\beta$  as a coiled-coil, as previously predicted (191, 192). The second helix in  $\gamma$  overlays the fifth and sixth blades of  $\beta$ ; the C-terminal loop of  $\gamma$  is buried, in part, in a hydrophobic pocket on the surface of  $\beta$ . The positions of direct (193) or chemically mediated intersubunit Cys cross-links (194) reflect proximity between the interhelical segment of  $\gamma$  and a segment of  $\beta$  that lies between its N-terminal helix and its first WD repeat, as also observed in the crystal structures. Mutagenesis experiments show that the coiled-coil contact is required to stabilize the dimer (192), even though peptides corresponding to the amino termini of  $\beta$  and  $\gamma$  do not associate in solution (195).  $\beta$  subunits show most variation in their N-terminal sequences, but these residues do not appear to confer selectivity for particular  $\gamma$  isoforms (182). Experiments with chimeric molecules show that segments corresponding to the fifth and sixth WD repeats in  $\beta$  (196, 197), and the second helical segment in  $\gamma$  (198), may encode the elements of selectivity. In remarkable agreement with the structural data (187), site-directed mutagenesis identifies Phe-40 in  $\gamma_1$  as a determinant for its specific interaction with  $\beta_1$  (199).

Three-dimensional structures of heterotrimeric complexes (lacking all lipid modifications) of  $G_{i\alpha 1}\beta_1\gamma_2$  (186) and  $\beta_1\gamma_1$  with a  $G_{i\alpha}/G_{i\alpha 1}$  chimera (in which residues 216–294 of  $G_{i\alpha}$  were replaced with the corresponding residues 220–298 of  $G_{i\alpha 1}$ ) (212) show two major sites of contact between  $G_{i\alpha}$  and  $\beta_\gamma$  (Figure 7). In contrast to the  $G_{i\alpha 1} \cdot$  GDP complex, in which residues 8–30 form a compact microdomain with the C terminus, in the  $G_{i\alpha}\beta_\gamma$  heterotrimer, the N-terminal 30 residues of  $G_{i\alpha}$  unfold to an extended helix that docks along the side of the first propeller blade (WD 1 and 2) of  $\beta$  (Figure 5). This contact, which buries about 900 Å<sup>2</sup> of solvent-accessible surface, contributes substantially to the interaction; indeed, truncation of the N terminus of  $G_{i\alpha}$  (118, 200),  $G_{o\alpha}$  (201, 202),  $G_{i\alpha 1}$  (201, 202), and  $G_{s\alpha}$  (203) abrogates their ability to bind  $\beta\gamma$ . Likewise, deletion of residues 7–10 (Glu-Glu-Arg, which is well conserved in the  $G_{i\alpha}$  family),

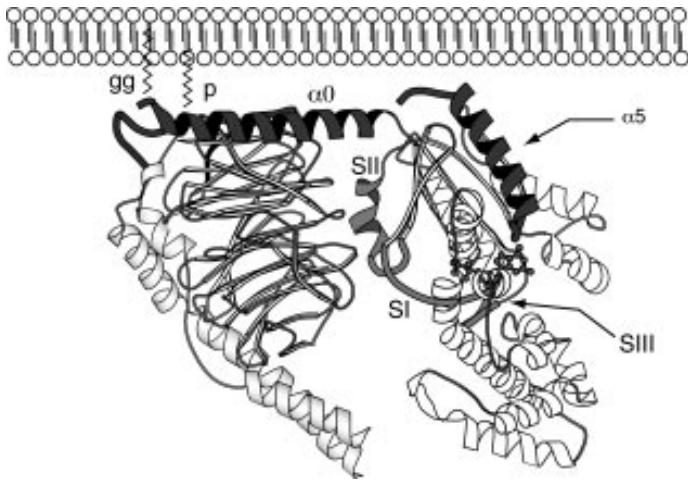


*Figure 7* The  $G_{i\alpha 1}\beta_1\gamma_2$  heterotrimer (186) (PDB entry 1GG2); the complex is shown with the proposed plasma membrane binding surface (212) oriented toward a model of the membrane bilayer. The geranylgeranyl (gg) group linked to the  $\gamma$ -subunit and the palmitoyl group (p) linked to  $G_{\alpha}$  are depicted with wavy lines. Surfaces of the heterotrimer that are proposed to contact cytoplasmic polypeptide loops of the receptor (not shown) are darkened and labeled, and the switch regions of the  $G_{i\alpha 1}$  subunit are shaded gray and labeled. The  $\beta_1\gamma_1$  dimer is also shaded. Bound GDP is shown as a ball-and-stick model.

but curiously, not substitution by Gln-Gln-Gln, prevents interaction with  $\beta\gamma$ . These three residues are not well ordered in the heterotrimer structures and do not appear to contribute substantially to the intersubunit contacts.  $G_{i\alpha 2}$ ,  $G_{z\alpha}$ , and  $G_{12\alpha}$  can be phosphorylated by protein kinase C (PKC) both in vitro and in cultured cells (see 204, 205, and references therein). This phosphorylation is inhibited by  $\beta\gamma$ ; conversely,  $G_{\alpha}$  subunits phosphorylated by PKC fail to bind  $\beta\gamma$ . The PKC phosphorylation site is located near the N terminus and probably corresponds to Ser-16 in  $G_{i\alpha 1}$ , because this residue is both conserved among the  $G_{\alpha}$  subunits isoforms that are PKC substrates and is surrounded with basic residues in keeping with the PKC phosphorylation site consensus. Ser-16 is located in the  $\alpha$ -helix that forms part of the interface with the  $\beta\gamma$  dimer. These observations suggest a physical basis for possible PKC-mediated down-regulation of certain  $G_{\alpha}$  isoforms.

N-terminal myristoylation of  $G_{i\alpha}$  and  $G_{\alpha o}$  (206) is required for high-affinity binding to  $\beta\gamma$  subunits (207, 208), but its role in the interaction cannot be discerned from the current structures because the  $G_{\alpha}$  subunit in the heterotrimers lacks this modification. The C terminus of  $\gamma$  and the N terminus of  $\alpha$  are located within 15 Å of each other, suggesting that  $\gamma$  subunit prenyl group and the  $G_{\alpha}$

subunit myristoyl and/or palmitoyl (69) groups penetrate the plasma membrane at the same locus. It has been reported that  $G_{\alpha\alpha}$  interacts directly with  $\gamma_2$ , but not  $\gamma_1$ , in the absence of  $\beta$  subunits, and that the discriminatory residues lie within the N terminus of the  $\gamma$  subunit (209, 210). However, neither of the heterotrimer structures shows any evidence for significant  $\alpha$ - $\gamma$  contacts. It is possible that  $\gamma$  prenylation, which enhances  $\alpha$ - $\gamma$  complex formation (209), stabilizes intersubunit interactions that are not detected in the structures of the unmodified heterotrimers.

$\beta\gamma$  subunits prevent dissociation of GDP from  $G_{\alpha}$  and directly compete with effector binding by direct contacts with the N terminus (115) and switch II (110) of  $G_{\alpha}$ . Six of the seven WD repeats in  $\beta$  (mostly involving the BC and DA loops of each blade of the  $\beta$  propeller) contribute to this surface, which buries about 1800 Å<sup>2</sup> of solvent-accessible area. In  $\beta 1$ , the largely hydrophobic interaction is centered around Trp-99. Mutation of the corresponding Trp-136 to glycine in the  $\beta$  subunit of *Saccharomyces cerevisiae* (211) results in constitutive activation of the mating response pathway, as expected if the interaction between  $G_{\alpha}$  and  $\beta\gamma$  has been disrupted. The Glu-307 → Lys suppressor mutation in yeast  $G_{\alpha}$  (corresponding to Gln-184 in switch I of  $G_{i\alpha}$ ) is proposed to act by forming a new ion pair with Asp-133 in yeast  $\beta$  (212). Also consistent with the crystal structure is the ability of 1,6-bismaleimido-hexane to cross-link Cys-215 of  $G_{\alpha\alpha}$  to both Cys-204 and Cys-271 in the fourth and sixth WD repeats of  $\beta 1$ , respectively (194, 213). The  $\beta\gamma$  contact protects all but one (the loop connecting the second and third WD repeats) of the trypsin-sensitive sites of  $\beta$ . Trypsin cleavage of the heterodimer at this site leaves a 27-kDa  $\beta$ -derived fragment that retains the ability to bind to  $G_{\alpha\alpha}$  (214).

The conformation of the switch II region is the same in both heterotrimer structures (186, 212) but quite different from that observed in either the GDP · Mg<sup>2+</sup>- (20), GDP- (22), or GTP $\gamma$ S · Mg<sup>2+</sup>-bound (19, 21) forms of the  $G_{\alpha}$  subunits (Figure 3). It appears that  $\beta\gamma$  remodels switch II, which otherwise adopts a completely disordered state in uncomplexed  $G_{i\alpha 1}$  · GDP subunits. In the  $\beta\gamma$ -bound conformation of  $G_{i\alpha 1}$ , both switch I and switch II—the Mg<sup>2+</sup> and GTP  $\gamma$ -phosphate binding sites—are dismantled, and a new ion pair between Arg-178 (G-2) and Glu-43 (G-3) traps GDP in its binding pocket (186). Release of GDP and its replacement by GTP triggers the dissociation of  $G_{\alpha}$  from  $\beta\gamma$ . However, mutation of Gly-226 to Ala in  $G_{s\alpha}$  blocks the GTP-dependent conformational change that effects  $\beta\gamma$  release (80, 102). The corresponding mutation in  $G_{i\alpha 1}$  [G203A (103)] has been exploited to develop an affinity reagent for the purification of soluble  $\beta\gamma$  subunits (176). Heterotrimers incorporating G203A  $G_{i\alpha 1}$  are virtually identical in structure to those containing wild-type  $G_{\alpha 1}$  (186). Model building suggests that the  $\beta$ -methyl substituent of Ala-203 generates unfavorable steric interactions, such that transition from the  $G_{\alpha}$  ·

GTP ·  $\beta\gamma$  complex to the GTP ·  $Mg^{2+}$ -bound state of free  $G_\alpha$  is energetically unfavorable.

A proposal for the mechanism by which small G-protein GDIs act was inspired by the structure of bovine brain  $\alpha$ -GDI (214a). This Rab-specific GDI binds specifically to the GDP-bound form of Rab and appears to be essential for the recycling of this small G protein between exocytic and endocytic compartments in vitro (214b). The three-dimensional fold of Rab-GDI has remarkable similarity to  $\alpha/\beta$  proteins of the flavodoxin family. Wu et al (214b) propose that a small parallel  $\beta$  sheet of GDI docks against the  $\beta 2$  strand of Rab, in a fashion reminiscent of the RapA1 · Raf-1RBD complex described above. Whether such a complex forms, and how it stabilizes the GDP-bound form of Rab, must await the structure of the complex.

### *GEFs of the Ras Family*

For most G proteins (EF-G is a notable exception), the reactivation step is catalyzed by a specific GEF that facilitates the release of the tightly bound GDP and its replacement by GTP. For example, the SOS, CDC25, and Vav proteins serve as such factors for Ras (158b, 215). These molecules apparently act by stabilizing the nucleotide-free form of Ras proteins (158b). The structure of human Mss4, a GEF for the Sec4/Ypt1/Rab branch of the Ras superfamily, has been determined by multi-dimensional NMR (215a). The structure of Mss4 comprises an antiparallel  $\beta$  sheet; two  $\beta$ -hairpin loops, each containing a CXXC motif, emanate from opposite ends of the sheet and coordinate a  $Zn^{2+}$  ion. Chemical shift changes upon formation of the Mss4 · Rab3a complex indicated that the C-terminal  $Zn^{2+}$ -binding loop, and a neighboring loop arising from the central region of the sheet, are likely both Rab3a binding sites. It is proposed that Mss4 binds to a highly conserved (within the Rab class of small G proteins) region preceding the G-3 box. The mechanism by which Mss4 stabilizes the nucleotide-free form of Rab3a is not yet apparent, but it is likely that the Ras-specific GEFs such as SOS and CDC25, which do not contain CXXC motifs, must bind Ras in a different manner from that proposed for the Rab3a · Mss4 complex.

Like the small G protein GEFs, ligand-activated, heptahelical G protein-coupled receptors must stabilize the nucleotide-free form of  $G_\alpha$ , which might be considered the transition state for the nucleotide exchange reaction. Intracellular guanine nucleotide concentrations are sufficient to saturate  $G_\alpha$ , and the GTP:GDP ratio is sufficiently high to ensure that the GTP-bound species predominates after a receptor-catalyzed exchange event. The reaction is kinetically irreversible because binding of GTP induces a conformational change in  $G_\alpha$  that causes it to be released from  $\beta\gamma$  (186, 212). Because  $\beta\gamma$  is required to stabilize the receptor- $G_\alpha$  interface (217), after  $G_\alpha$  dissociates,  $G_\alpha$

cannot re-engage the receptor until GTP hydrolysis occurs and a heterotrimer is reformed. Membrane-proximal residues in the second and third cytoplasmic-facing loops of G protein-coupled receptors, together with the C-terminal tail of such receptors, play a role in heterotrimer recognition and in catalysis of nucleotide exchange (55, 216). Despite the apparent selectivity of some G protein/receptor pairings (for example,  $\beta$ -adrenergic receptors couple only with  $G_s$ , whereas muscarinic receptors interact only with  $G_i$  and  $G_q$ ), the inherent specificity of heterotrimer/receptor interactions is limited, as shown by the first reconstitution experiments (208, 218). This inherent limitation is reflected in the length and sequence diversity of the receptor cytoplasmic loops implicated in heterotrimer recognition (219). Nevertheless, receptors exhibit preferences for certain  $\beta\gamma$  subtypes (220–223), which may be dictated by a C-terminal region in the  $\gamma$  subunit (224). Other factors, including cellular compartmentation (125) and synergism between  $\beta\gamma$  and  $\alpha$  subunits (56, 172), may influence the ultimate specificity of receptor-heterotrimer coupling. Although it is not surprising that receptor-derived peptides are capable of blocking receptor-heterotrimer interactions and that they do so synergistically, it is interesting that a variety of such peptides can catalyze nucleotide exchange (225). Further, even nonreceptor-derived peptides, such as the wasp venom mastoparans (226), can act as GEFs for heterotrimers. Most active peptides are short (10–26 amino acids) and cationic, but they vary in sequence, hydrophobicity, amphiphilicity, and helical content (225). Therefore, peptides either interact at different sites on the heterotrimer, as suggested by the fact that different peptides can act synergistically (227), or the exchange mechanism itself does not depend upon a sequence-specific interaction at the receptor-heterotrimer binding site. Neither possibility is compatible with a model in which the GDP-binding site is emptied by disengagement of a discrete molecular latch on the heterotrimer. In addition to its GEF activity, the receptor must also serve as a chaperone to stabilize the transient but unstable “empty” state of  $G_\alpha$ .

A site (or several sites) on the heterotrimer must contact the receptor (Figure 7). The C-terminus of  $G_\alpha$  is probably one such region (see 228 for a detailed discussion). Because C-terminal truncations of  $G_\alpha$  subunits reduce their affinity for GDP, it has been proposed that a receptor may act by perturbing the C-terminal helix to promote release of GDP from its binding pocket (172). The G-5-containing loop (Table 1) between strand  $\beta 6$  and the C-terminal helix ( $\alpha 5$ ) has also been proposed to be a receptor contact site. Peptides corresponding to this region are potent inhibitors of receptor-mediated nucleotide exchange (229). Certain mutations within this loop, notably the A366S  $G_{s\alpha}$  associated with pseudohypoparathyroidism/testotoxicosis, cause an 80-fold increase in the rate of GDP release (230). Such mutations might, to a degree, simulate the conformation of  $G_\alpha$  induced by the receptor. Cross-linking of an  $\alpha 2$  adrenergic

receptor-derived peptide to the N terminus of  $G_{i\alpha 1}$  and to a site in the  $\beta$  subunit (231) also implicates these two regions as potential receptor interaction sites. When mapped upon the molecular surface of the heterotrimer, the potential receptor contact regions define an extended and partially interconnected surface (Figure 5). Lambright et al (212) propose that a relatively flat hydrophobic surface of the heterotrimer formed by the N terminus of  $G_{i\alpha}$  and adjacent surfaces of the  $\beta\gamma$  subunit contacts the membrane. In the refined structure of the  $G_{i\alpha 1} \cdot \beta_1\gamma_2$ , we have noticed a positively charged region near the N terminus of  $G_{i\alpha 1}$  that could contact the phospholipid headgroups of the lipid surface. With the heterotrimer so juxtaposed to the membrane, several of the proposed receptor interaction sites would be accessible to segments of the receptor emerging from the membrane. Most notable in this model is the negatively charged cavity at the  $\alpha_{i\alpha 1}/\beta_1$  interface. Cationic loops or helical regions of the receptor binding at this site would have clear access to the switch regions and could thus perturb the nucleotide-binding site. Simultaneously, receptor sequences interacting with the  $G_{i\alpha}$  subunit near the  $\alpha 5$  and  $\alpha 4$ - $\beta 6$  surface could destabilize nucleotide binding from the "back side" of the nucleotide-binding pocket.

### *Elongation Factor Ts*

The complex of EF-Tu · EF-Ts (233) may, to some degree, serve as a model for the mechanism by which G protein-coupled receptors, and GEFs in general, catalyze nucleotide exchange. EF-Ts recognizes a conformation of EF-Tu that is similar to the free GDP complex and interposes a Phe residue between His-85 of the switch II helix and His-118 in the  $\alpha 3$  helix. This intrusion displaces the  $\alpha 2$  helix, which in turn destroys the  $Mg^{2+}$ -binding site by dislocating the Asp in G-3. Because GDP is bound tightly only in the presence of  $Mg^{2+}$ , the nucleotide is able to diffuse away. EF-Ts perturbs guanine ring binding at the NXLD site, thereby loosening the grip of Tu on the base. EF-Ts also induces a flip in the peptide bond between Val-20 and Asp-21 that destabilizes GDP, but not GTP, binding. Some aspects of the EF-Ts mechanism might apply to G protein-coupled receptors, but the destabilization of the  $Mg^{2+}$ -binding site is unlikely to be one of them. The  $Mg^{2+}$  site is empty in GDP-bound heterotrimers. In fact, millimolar  $Mg^{2+}$  concentrations actually cause nucleotide exchange in G protein heterotrimers (226). On the other hand, Ras GEFs may well employ an EF-Ts-like mechanism.

## SUMMARY

The complex molecular machinery that constitutes a G protein regulatory apparatus is focused on the conformation of a single structural element common to all G proteins: the switch II helix. This element of chemomechanical energy

transduction is tensioned in a high energy state by the binding of GTP. In this state, a G protein binds its cognate target effector. When GTP is hydrolyzed, energy is dissipated with the collapse of switch II and the effector is released. Members of the G protein superfamily that depend upon the action of GAPs in order to catalyze GTP hydrolysis behave as switches; those, like the translation elongation factors that hydrolyze GTP only when bound in a ternary complex to the ribosome and the correct AA-tRNA, act as sensors or proofreaders; finally, G proteins that rely on their intrinsic catalytic activity become clocks. The work described above has begun to elucidate some of the mechanisms by which the rate of GTP hydrolysis is regulated. The challenges that remain for the future are to discover how the energy of GTP-binding is deployed in effector recognition, and how G proteins, once the energy of hydrolysis is spent, are restored to the high-energy, GTP-bound state through the action of nucleotide exchange factors.

#### ACKNOWLEDGMENTS

I am indebted to Alfred Gilman for his wisdom, collegiality, and collaboration over the years. I am grateful also to the many colleagues in both our laboratories who have contributed to some of the work described here; to David Coleman, Mark Wall, and Mark Mixon for assistance with preparing the figures; and to Morten Kjeldgaard for coordinates of EF-Tu. Research has been supported in part by grants from the NIH #DK46371, the Welch foundation #I-1229, and the Howard Hughes Medical Institute.

Visit the *Annual Reviews* home page at  
<http://www.annurev.org>.

#### Literature Cited

1. Bourne HR, Sanders DA, McCormick F. 1990. *Nature* 348:125–32
- 1a. Kjeldgaard M, Nyborg J, Clark BFC. 1996. *FASEB J.* 10:1347–68
2. Bourne HR, Sanders DA, McCormick F. 1991. *Nature* 349:117–27
3. Morikawa K, La Cour TFM, Nyborg J, Rasmussen KM, Miller DL, Clark BFC. 1978. *J. Mol. Biol.* 125:325–38
4. Jurnak F, McPherson A, Wang AHJ, Rich A. 1980. *J. Biol. Chem.* 255:6751–57
5. Jurnak F. 1985. *Science* 230:32–36
6. La Cour TFM, Nyborg J, Thirup S, Clark BFC. 1985. *EMBO J.* 4:2385–88
7. Brändén C-I. 1980. *Q. Rev. Biophys.* 13:317–38
8. Dever TE, Glynias MJ, Merrick WC. 1987. *Proc. Natl. Acad. Sci. USA* 84: 1814–18
9. Halliday KR. 1984. *J. Cycl. Nucleotide Protein Phosphoryl. Res.* 9:435–48
10. McCormick F, Clark BFC, La Cour TFM, Kjeldgaard M, Nørskov-Lauritsen L, Nyborg J. 1985. *Science* 230:78–82
11. Gilman AG. 1987. *Annu. Rev. Biochem.* 56:615–49
12. Möller W, Amons R. 1985. *FEBS Lett.* 186:1–7
13. Walker JE, Saraste M, Runswick MJ, Gay NJ. 1982. *EMBO J.* 1:945–51
14. Pai EF, Kregel U, Petsko GA, Goody RS, Kabsch W, Wittinghofer A. 1990. *EMBO J.* 9:2351–59

15. Tong L, de Vos AM, Milburn MV, Kim S-H. 1991. *J. Mol. Biol.* 217:503-16
16. Kjeldgaard M, Nissen P, Thirup S, Nyborg J. 1993. *Structure* 1:35-50
17. Berchtold H, Reshetnikova L, Reiser COA, Schirmer NK, Sprinzl M, Hilgenfeld R. 1993. *Nature* 365:126-32
18. Kjeldgaard M, Nyborg J. 1992. *J. Mol. Biol.* 223:721-42
- 18a. Polekhina G, Thirup S, Kjeldgaard M, Nissen P, Lippmann C, Nyborg J. 1996. *Structure* 4:1141-51
19. Noel JP, Hamm HE, Sigler PB. 1993. *Nature* 366:654-63
20. Lambright DG, Noel JP, Hamm HE, Sigler PB. 1994. *Nature* 369:621-28
21. Coleman DE, Berghuis AM, Lee E, Linder ME, Gilman AG, Sprang SR. 1994. *Science* 265:1405-12
22. Mixon MB, Lee E, Coleman DE, Berghuis AM, Gilman AG, Sprang SR. 1995. *Science* 270:954-60
23. Barbacid M. 1987. *Annu. Rev. Biochem.* 56:779-827
24. Nuoffer C, Balch WE. 1994. *Annu. Rev. Biochem.* 63:949-90
25. Macara IG, Lounsbury KM, Richards SA, McKiernan C, Bar-Sagi D. 1996. *FASEB J.* 10:625-30
26. Grand RJA, Owen D. 1991. *Biochem. J.* 279:609-31
27. Tong L, Milburn MV, de Vos AM, Kim S-H. 1989. *Science* 245:244
28. Pai EF, Kabsch W, Krengel U, Holmes KC, John J, Wittinghofer A. 1989. *Nature* 341:209-14
29. de Vos AM, Tong L, Milburn MV, Matias PM, Jancarik J, et al. 1988. *Science* 239:888-93
30. Milburn MV, Tong L, deVos AM, Brünger A, Yamaizumi Z, et al. 1990. *Science* 247:939-45
31. Privé GG, Milburn MV, Tong L, deVos AM, Yamaizumi Z, et al. 1992. *Proc. Natl. Acad. Sci. USA* 89:3649-53
32. Schlichting I, Almo SC, Rapp G, Wilson K, John J, et al. 1990. *Nature* 345:309-15
33. Krengel U, Schlichting I, Scherer A, Schumann R, Frech M, et al. 1990. *Cell* 62:539-48
34. Scheidig AJ, Franken SM, Corrie JET, Reid GP, Wittinghofer A, et al. 1995. *J. Mol. Biol.* 253:132-50
35. John J, Schlichting I, Schiltz E, Rösch P, Wittinghofer A. 1989. *J. Biol. Chem.* 264:13086-92
36. Casey PJ. 1995. *Science* 268:221-25
37. Marshall MS. 1993. *Trends Biochem. Sci.* 18:250-54
38. Kraulis PJ, Domaille PJ, Campbell-Burk SL, Van Aken T, Laue ED. 1994. *Biochemistry* 33:3515-31
39. Nassar M, Horn G, Herrmann C, Scherer A, McCormick F, Wittinghofer A. 1995. *Nature* 375:554-60
40. Schlenstedt G. 1966. *FEBS Lett.* 389:75-79
- 40a. Scheffzek K, Klebe C, Fritz-Wolf K, Kabsch W, Wittinghofer A. 1995. *Nature* 374:378-81
41. Amor JC, Harrison DH, Kahn DH, Ringe D. 1994. *Nature* 372:704-8
42. Greasley SE, Jhoti H, Teahan C, Solari R, Fensome A, et al. 1995. *Nat. Struct. Biol.* 2:797-806
43. Kahn RA, Gilman AG. 1986. *J. Biol. Chem.* 261:7906-11
44. Rothman JE. 1994. *Nature* 372:55-63
45. Brown HA, Gutowski S, Moomaw CR, Slaughter C, Sternweis PC. 1993. *Cell* 75:1137-44
46. Abel K, Jurnak F. 1996. *Structure* 4:229-38
47. Peter ME, Schirmer NK, Reiser COA, Sprinzl M. 1990. *Biochemistry* 29:2876-84
- 47b. Abel K, Yoder MD, Hilgenfeld R, Jurnak F. 1996. *Structure* 4:1153-59
48. Aevansson A, Brazhnikova E, Garber M, Zheltonosova J, Chirgadze Y, et al. 1994. *EMBO J.* 13:3669-77
49. Czworkowski J, Wang J, Steitz TA, Moore PB. 1994. *EMBO J.* 13:3661-68
50. Nissen P, Kjeldgaard M, Thirup S, Polekhina G, Reshetnikova L, et al. 1995. *Science* 270:1464-72
51. Moore PB. 1995. *Science* 270:1453-54
52. Kaziro Y, Itoh H, Kozasa T, Nakafuku M, Satoh T. 1991. *Annu. Rev. Biochem.* 60:349-400
53. Hamm HE, Gilchrist A. 1996. *Curr. Opin. Cell Biol.* 8:189-96
54. Rens-Domiano S, Hamm HE. 1995. *FASEB J.* 9:1059-66
55. Helmreich E, Hofmann K-P. 1996. *Biochem. Biophys. Acta* 1286:285-322
56. Sunahara RK, Dessauer CW, Gilman AG. 1996. *Annu. Rev. Pharmacol. Toxicol.* 36:461-80
57. Markby DW, Onrust R, Bourne HR. 1993. *Science* 262:1895-901
58. Benjamin DR, Markby DW, Bourne HR, Kuntz ID. 1995. *J. Mol. Biol.* 254:681-91
59. Freissmuth M, Gilman AG. 1989. *J. Biol. Chem.* 264:21907-14
60. Landis CA, Masters SB, Spada A, Pace AM, Bourne HR, Vallar L. 1989. *Nature* 340:692-96

61. Antonelli M, Birnbaumer L, Allende JE, Olate J. 1994. *FEBS Lett.* 340:249–54
62. Linder ME, Middleton P, Hepler JR, Taussig R, Gilman AG, Mumby SM. 1993. *Proc. Natl. Acad. Sci. USA* 90:3675–79
63. Wedegaertner PB, Chu DH, Wilson PT, Levis MJ, Bourne HR. 1993. *J. Biol. Chem.* 268:25001–8
64. Veit M, Nürnberg B, Spicher K, Harteneck C, Ponimaskin E, et al. 1994. *FEBS Lett.* 339:160–64
65. Gallego C, Gupta SK, Winitz S, Eisfelder BJ, Johnson GL. 1992. *Proc. Natl. Acad. Sci. USA* 89:9695–99
66. Wilson PT, Bourne HR. 1995. *J. Biol. Chem.* 270:9667–75
67. Wedegaertner PB, Bourne HR. 1994. *Cell* 77:1063–70
68. Mumby SM, Kleuss C, Gilman AG. 1994. *Proc. Natl. Acad. Sci. USA* 91:2800–4
69. Wedegaertner PB, Wilson PT, Bourne HR. 1995. *J. Biol. Chem.* 270:503–6
70. Milligan G, Parenti M, Magee AI. 1995. *Trends Biochem. Sci.* 20:181–86
71. Van Dop C, Tsubokawa M, Bourne HR, Ramachandran J. 1984. *J. Biol. Chem.* 259:696–98
72. John J, Sohmen R, Feuerstein J, Linke R, Wittinghofer A, Goody RS. 1990. *Biochemistry* 29:6058–65
73. Feuerstein J, Kalbitzer HR, John J, Goody RS, Wittinghofer A. 1987. *Eur. J. Biochem.* 162:49–55
74. Feuerstein J, Goody RS, Wittinghofer A. 1987. *J. Biol. Chem.* 262:8455–58
75. Ferguson KM, Higashijima T, Smigel MD, Gilman AG. 1986. *J. Biol. Chem.* 261:7393–99
76. Goody RS, Frech M, Wittinghofer A. 1991. *Trends Biochem. Sci.* 16:327–28
77. Arai K-I, Arai N, Nakamura S, Oshima T, Kaziro Y. 1978. *Eur. J. Biochem.* 92:521–31
78. Wagner A, Simon I, Sprinzl M, Goody RS. 1995. *Biochemistry* 34:12535–42
79. Higashijima T, Ferguson KM, Sternweis PC, Smigel MD, Gilman AG. 1987. *J. Biol. Chem.* 262:762–66
80. Lee E, Taussig R, Gilman AG. 1992. *J. Biol. Chem.* 267:1212–18
81. Northup JK, Smigel MD, Gilman AG. 1982. *J. Biol. Chem.* 257:11416–23
82. Higashijima T, Ferguson KM, Sternweis PC, Ross EM, Smigel MD, Gilman AG. 1987. *J. Biol. Chem.* 262:752–56
83. John J, Frech M, Wittinghofer A. 1988. *J. Biol. Chem.* 263:11792–99
84. Arai K-I, Kawakita M, Kaziro Y. 1972. *J. Biol. Chem.* 247:7029–37
85. John J, Rensland H, Schlichting I, Vetter I, Borasio GD, et al. 1993. *J. Biol. Chem.* 268:923–29
86. Fawzi AB, Northup JK. 1990. *Biochemistry* 29:3804–12
87. Casey PJ, Fong HK, Simon MI, Gilman AG. 1990. *J. Biol. Chem.* 265:2383–90
88. Hepler JR, Kozasa T, Smrcka AV, Simon MI, Rhee SG, et al. 1993. *J. Biol. Chem.* 268:14367–75
89. Franken SM, Scheidig AJ, Krenzel U, Rensland H, Lautwein A, et al. 1993. *Biochemistry* 32:8411–20
90. Slepak VZ, Quick MW, Aragay AM, Davidson N, Lester HA, Simon MI. 1993. *J. Biol. Chem.* 268:21889–94
91. Slepak VZ, Katz A, Simon MI. 1995. *J. Biol. Chem.* 270:4037–41
92. Denker BM, Neer EJ, Schmidt CJ. 1992. *J. Biol. Chem.* 267:6272–77
93. Denker BM, Boutin PM, Neer EJ. 1995. *Biochemistry* 34:544–53
94. Rensland H, Linke JR, Simon I, Schlichting I, Wittinghofer A, Goody RS. 1995. *Biochemistry* 34:593–99
95. Zhong JM, Chen-Hwang MC, Hwang YW. 1995. *J. Biol. Chem.* 270:10002–7
96. Hwang Y-W, Miller DL. 1987. *J. Biol. Chem.* 262:13081–85
97. Schmidt G, Lenzen C, Simon I, Deuter R, Cool RH, et al. 1996. *Oncogene* 12:87–96
98. Weijland A, Parlato G, Parmeggiani A. 1994. *Biochemistry* 33:10711–17
99. Neal SE, Eccleston JF, Webb MR. 1990. *Proc. Natl. Acad. Sci. USA* 87:3562–65
100. Stouten PFW, Sander C, Wittinghofer A, Valencia A. 1993. *FEBS Lett.* 320:1–6
101. Sung Y-J, Carter M, Zhong J-M, Hwang Y-W. 1995. *Biochemistry* 34:3470–77
102. Miller RT, Masters SB, Sullivan KA, Beiderman B, Bourne HR. 1988. *Nature* 334:712–15
103. Berghuis AM, Lee E, Raw AS, Gilman AG, Sprang SR. 1996. *Structure*. In press
104. Hwang YW, Journak F, Miller DL. 1989. In *The Guanine-Nucleotide Binding Proteins: Common Structural and Functional Properties*, ed. L Bosch, B Kraal, A Parmeggiani, pp. 77–85. New York: Plenum
105. Polakis P, McCormick F. 1993. *J. Biol. Chem.* 268:9157–60
106. Marshall M. 1995. *Mol. Reprod. Dev.* 42:493–99
107. Cook SJ, Rubinfeld B, Albert I, McCormick F. 1993. *EMBO J.* 12:3475–85

108. Emerson SD, Madison VS, Palermo RE, Waugh DS, Scheffler JE, et al. 1995. *Biochemistry* 34:6911–18
109. Block C, Janknecht R, Herrmann C, Nassar N, Wittinghofer A. 1996. *Nat. Struct. Biol.* 3:244–51
- 109a. Sprang ST. 1995. *Structure* 3:641–43
- 109b. Wittinghofer A, Nassar N. 1996. *Trends Biochem. Sci.* 21:488–91
- 109c. Scheffzek K, Lautwein A, Kabsch W, Ahmadian MR, Wittinghofer A. 1996. *Nature* 384:591–96
110. Berlot CH, Bourne HR. 1992. *Cell* 68:911–22
111. Itoh H, Gilman AG. 1991. *J. Biol. Chem.* 266:16226–31
112. Rarick H, Artemyev NO, Hamm HE. 1992. *Science* 256:1031–33
113. Faurobert E, Otto-Bruc A, Chardin P, Chabre M. 1993. *EMBO J.* 12:4191–98
114. Skiba NP, Bae H, Hamm HE. 1996. *J. Biol. Chem.* 271:413–24
115. Hepler JR, Biddlecome GH, Kleuss C, Camp LA, Hofmann SL, et al. 1996. *J. Biol. Chem.* 271:496–504
116. Mittal R, Erickson JW, Cerione RA. 1996. *Science* 271:1413–16
117. Phillips WJ, Cerione RA. 1986. *J. Biol. Chem.* 263:15498–505
118. Fung BK-K, Nash CR. 1983. *J. Biol. Chem.* 258:10503–10
119. Hurley JB, Simon MI, Teplow DB, Robshaw JD, Gilman AG. 1984. *Science* 226:860–62
120. Nakamura S-I, Rodbell M. 1991. *Proc. Natl. Acad. Sci. USA* 88:7150–54
121. Vaillancourt RR, Dhanasekaran N, Johnson GL, Ruoho AE. 1990. *Proc. Natl. Acad. Sci. USA* 87:3645–49
122. Vaillancourt RR, Dhanasekaran N, Ruoho AE. 1995. *Biochem. J.* 311:987–93
123. Rodbell M. 1992. *Curr. Top. Cell. Regul.* 32:1–47
124. Bourne HR. 1995. *Science* 270:933–34
125. Neubig RR. 1994. *FASEB J.* 8:939–46
126. Lisanti MP, Scherer PE, Tang Z, Sargiacomo M. 1994. *Trends Cell Biol.* 4:231–35
127. Temeles GL, Gibbs JB, D'Alonzo JS, Sigal IS, Scolnick EM. 1985. *Nature* 313:700–3
128. Kalbitzer HR, Goody RS, Wittinghofer A. 1984. *Eur. J. Biochem.* 141:591–97
129. Webb MR, Eccleston JF. 1981. *J. Biol. Chem.* 256:7734–37
130. Eccleston JF, Webb MR. 1982. *J. Biol. Chem.* 257:5046–49
131. Feuerstein J, Goody RS, Webb MR. 1989. *J. Biol. Chem.* 264:6188–90
132. Der CJ, Finkel T, Cooper GM. 1986. *Cell* 44:167–76
133. Vogel US, Dixon RAF, Schaber MD, Diehl RE, Marshall MS, et al. 1988. *Nature* 335:90–93
134. Graziano MP, Gilman AG. 1989. *J. Biol. Chem.* 264:15475–82
135. Lyons J, Landis CA, Harsh G, Vallar L, Grünewald K, et al. 1990. *Science* 249:655–59
136. Frech M, Darden TA, Pedersen LG, Foley CK, Charifson PS, et al. 1994. *Biochemistry* 33:3237–44
137. Langen R, Schweins T, Warshel A. 1992. *Biochemistry* 31:8691–96
138. Chung H-H, Benson DR, Schultz PG. 1993. *Science* 259:806–9
139. Kleuss C, Raw AS, Lee E, Sprang SR, Gilman AG. 1994. *Proc. Natl. Acad. Sci. USA* 91:9828–31
140. Schweins T, Langen R, Warshel A. 1994. *Nat. Struct. Biol.* 1:476–84
141. Schweins T, Geyer M, Scheffzek K, Warshel A, Kalbitzer HR, Wittinghofer A. 1995. *Nat. Struct. Biol.* 2:36–44
142. Sternweis PC, Gilman AG. 1982. *Proc. Natl. Acad. Sci. USA* 79:4888–91
143. Bigay J, Deterre P, Pfister C, Chabre M. 1985. *FEBS Lett.* 191:181–85
144. Antonny B, Chabre M. 1992. *J. Biol. Chem.* 267:6710–18
145. Martin RB. 1996. *Coord. Chem. Rev.* 141:23–42
146. Sondek J, Lambright DG, Noel JP, Hamm HE, Sigler PB. 1994. *Nature* 372:276–79
147. Cassel D, Selinger Z. 1977. *Proc. Natl. Acad. Sci. USA* 74:3307–11
148. Kahn RA. 1991. *J. Biol. Chem.* 266:15595–97
149. Kraal B, de Graaf MJ, Mesters JR, van Hoof PJM, Jaacquet E, Parmeggiani A. 1990. *Eur. J. Biochem.* 192:305–9
150. Codina J, Birnbaumer L. 1994. *J. Biol. Chem.* 269:29339–42
151. Rensland H, Lautwein A, Wittinghofer A, Goody RS. 1991. *Biochemistry* 30:11181–85
152. Cool RH, Parmeggiani A. 1991. *Biochemistry* 30:362–66
153. Maegley KA, Admiraal SJ, Herschlag D. 1996. *Proc. Natl. Acad. Sci. USA* 93:8160–66
154. Trahey M, McCormick F. 1987. *Science* 238:542–45
155. Gideon P, John J, Frech M, Lautwein A, Clark R, et al. 1992. *Mol. Cell. Biol.* 12:2050–56
156. Eccleston JF, Moore KJM, Morgan L, Skinner RH, Lowe PN. 1993. *J. Biol. Chem.* 268:27012–19

157. Mittal R, Ahmadian MH, Goody RS, Wittinghofer A. 1996. *Science* 273:115–17
158. Skinner RH, Bradley S, Brown AL, Johnson NJE, Rhodes S, et al. 1991. *J. Biol. Chem.* 266:14163–66
- 158a. Musacchio A, Cantley LC, Harrison SC. 1996. *Proc. Natl. Acad. Sci. USA* 93:14373–78
- 158b. Boguski MS, McCormick. 1993. *Nature* 366:643–54
159. Berstein G, Blank JL, Jhon D-Y, Exton JH, Rhee SG, Ross EM. 1992. *Cell* 70:411–18
160. Biddlecome GH, Berstein G, Ross EM. 1996. *J. Biol. Chem.* 271:7999–8007
161. Arshavsky VY, Dumke CL, Zhu Y, Artemyev NO, Skiba NP, et al. 1994. *J. Biol. Chem.* 269:19882–87
162. Ross EM. 1996. *Recent Prog. Horm. Res.* 50:207–21
163. Druey KM, Blumer KJ, Kang VH, Kehrl JH. 1996. *Nature* 379:742–46
164. Dohlman HG, Song JP, Ma D, Courchesne WE, Thorner J. 1995. *Mol. Cell. Biol.* 16:5194–209
165. Koelle MR, Horvitz HR. 1996. *Cell* 84:115–25
166. De Vries L, Mousli M, Wurmsler A, Farquhar MG. 1995. *Proc. Natl. Acad. Sci. USA* 92:11916–20
167. Berman DM, Wilke TM, Gilman AG. 1996. *Cell* 86:1–20
168. Watson N, Linder ME, Druey KM, Kehrl JH, Blumer KJ. 1996. *Nature* 383:172–75
169. Hunt TW, Fields TA, Casey PJ, Peralta EG. 1996. *Nature* 383:175–77
170. Berman DM, Kozasa T, Gilman AG. 1996. *J. Biol. Chem.* 271:27209–12
- 170a. Clapham DE, Neer EJ. 1993. *Nature* 365:403–6
171. Sternweis PC. 1994. *Curr. Opin. Cell Biol.* 6:198–203
172. Neer EJ. 1995. *Cell* 80:249–57
173. Watson AJ, Katz A, Simon MI. 1994. *J. Biol. Chem.* 269:22150–56
174. Ray K, Kunsch C, Bonner LM, Robishaw JD. 1995. *J. Biol. Chem.* 270:21765–71
175. Hurley JB, Fong HKW, Teplow DB, Dreyer WJ, Simon MI. 1984. *Proc. Natl. Acad. Sci. USA* 81:6948–52
176. Ueda N, Iñiguez-Lluhi JA, Lee E, Smrcka AV, Robishaw JD, Gilman AG. 1994. *J. Biol. Chem.* 269:4388–95
177. Iñiguez-Lluhi JA, Simon MI, Robishaw JD, Gilman AG. 1992. *J. Biol. Chem.* 267:23409–17
178. Schmidt CJ, Neer EJ. 1991. *J. Biol. Chem.* 266:4538–44
179. Robishaw JD, Kalman VK, Proulx KL. 1992. *Biochem. J.* 286:677–80
180. Higgins JB, Casey PJ. 1994. *J. Biol. Chem.* 269:9067–72
181. Schmidt CJ, Thomas TC, Levine MA, Neer EJ. 1992. *J. Biol. Chem.* 267:13807–10
182. Pronin AN, Gautam N. 1992. *Proc. Natl. Acad. Sci. USA* 89:6220–24
183. Graf R, Mattera R, Codina J, Evans T, Ho Y-K, Estes MK, Birnbaumer L. 1992. *Eur. J. Biochem.* 210:609–19
184. Smrcka AV, Sternweis PC. 1993. *J. Biol. Chem.* 268:9667–74
185. Wickman KD, Iñiguez-Lluhi JA, Davenport PA, Taussig R, Krapivinsky GB, et al. 1994. *Nature* 368:255–57
186. Wall MA, Coleman DE, Lee E, Iñiguez-Lluhi JA, Posner BA, et al. 1995. *Cell* 83:1047–58
187. Sondek J, Bohm A, Lambright DG, Hamm HE, Sigler PB. 1996. *Nature* 379:369–74
- 187a. Murzin AG. 1992. *Proteins* 14:191–201
188. Fong HKW, Hurley JB, Hopkins RS, Miale-Lye R, Johnson MS, et al. 1986. *Proc. Natl. Acad. Sci. USA* 83:2162–66
189. Simon MI, Strathmann MP, Gautam N. 1991. *Science* 252:802–8
190. Neer EJ, Schmidt CJ, Nambudripad R, Smith TF. 1994. *Nature* 371:297–300
191. Lupas AN, Lupas JM, Stock JB. 1992. *FEBS Lett.* 314:105–8
192. Garritsen A, van Galen PJM, Simonds WF. 1993. *Proc. Natl. Acad. Sci. USA* 90:7706–10
193. Bubis J, Khorana HG. 1990. *J. Biol. Chem.* 265:12995–99
194. Garcia-Higuera I, Thomas TC, Yi F, Neer EJ. 1996. *J. Biol. Chem.* 271:528–35
195. Marin EP, Neubig RR. 1995. *Biochem. J.* 309:377–80
196. Garritsen A, Simonds WF. 1994. *J. Biol. Chem.* 269:24418–23
197. Katz A, Simon MI. 1995. *Proc. Natl. Acad. Sci. USA* 92:1998–2002
198. Spring DJ, Neer EJ. 1994. *J. Biol. Chem.* 269:22882–86
199. Lee CH, Murakami T, Simonds WF. 1995. *J. Biol. Chem.* 270:8779–84
200. Navon SE, Fung BK-K. 1987. *J. Biol. Chem.* 262:15746–51
201. Neer EJ, Pulsifer L, Wolf LG. 1988. *J. Biol. Chem.* 263:8896–9000
202. Graf R, Mattera R, Codina J, Estes M, Birnbaumer L. 1992. *J. Biol. Chem.* 267:24307–14

203. Journot L, Pantaloni C, Bockaert J, Audigier Y. 1991. *J. Biol. Chem.* 266:9009–15
204. Kozasa T, Gilman AG. 1996. *J. Biol. Chem.* 271:12562–12567
205. Fields TA, Casey PJ. 1995. *J. Biol. Chem.* 270:23119–25
206. Mumby SM, Heukeroth RO, Gordon JI, Gilman AG. 1990. *Proc. Natl. Acad. Sci. USA* 87:728–32
207. Linder ME, Pang IH, Duronio RJ, Gordon JI, Sternweis PC, Gilman AG. 1991. *J. Biol. Chem.* 266:4654–59
208. Cerione RA, Staniszewski C, Benovic JL, Lefkowitz RJ, Caron MG, et al. 1985. *J. Biol. Chem.* 260:1493–1500
209. Rahmatullah M, Robishaw JD. 1994. *J. Biol. Chem.* 269:3574–80
210. Rahmatullah M, Ginnan R, Robishaw JD. 1995. *J. Biol. Chem.* 270:2946–51
211. Whiteway M, Clark KL, Leberer E, Dignard D, Thomas DY. 1994. *Mol. Cell. Biol.* 14:3223–29
212. Lambright DG, Sondek J, Bohm A, Skiba NP, Hamm H, Sigler PB. 1996. *Nature* 379:311
213. Thomas TC, Schmidt CJ, Neer EJ. 1993. *Proc. Natl. Acad. Sci. USA* 90:10295–99
214. Thomas TC, Sladek T, Yi F, Smith T, Neer EJ. 1993. *Biochemistry* 32:8628–35
- 214a. Schalk I, Zeng K, Wu S-K, Stura E, Matteson J, et al. 1996. *Nature* 38:42–48
- 214b. Wu S-K, Zeng K, Wilson IA, Balch WE. 1996. *Trends Biochem. Sci.* 21:472–76
215. Overbeck AF, Brtva TR, Cox AD, Graham SM, Huff SY, et al. 1995. *Mol. Reprod. Dev.* 42:468–76
- 215a. Yu H, Schreiber SL. 1995. *Nature* 376:788–90
216. Strader CD, Fong TM, Tota MR, Underwood D, Dixon RAF. 1994. *Annu. Rev. Biochem.* 63:101–32
217. Phillips WJ, Cerione RA. 1992. *J. Biol. Chem.* 267:17032–39
218. Asano T, Katada T, Gilman AG, Ross EM. 1984. *J. Biol. Chem.* 259:9351–54
219. Watson S, Arkininstall S. 1996. *The G-Protein Linked Receptor Factsbook*, pp. 2–295. London: Academic
220. Kleuss C, Hescheler J, Ewel C, Rosenthal W, Schultz G, Wittig B. 1991. *Nature* 353:43–48
221. Kleuss C, Scherubl H, Hescheler J, Schultz G, Wittig B. 1992. *Nature* 358:424–26
222. Kleuss C, Scherubl H, Hescheler J, Schultz G, Wittig B. 1993. *Science* 259:832–34
223. Kisselev O, Gautam N. 1993. *J. Biol. Chem.* 268:24519–22
224. Kisselev OG, Ermolaeva MV, Gautam N. 1994. *J. Biol. Chem.* 269:21399–402
225. Taylor JM, Neubig RR. 1994. *Cell. Signal.* 6:841–49
226. Higashijima T, Burnier J, Ross EM. 1990. *J. Biol. Chem.* 265:14176–86
227. Wade SM, Dalman HM, Yang S-Z, Neubig RR. 1994. *Mol. Pharmacol.* 45:1191–97
228. Conklin BR, Bourne HR. 1993. *Cell* 73:631–41
229. Rasenick MM, Watanabe M, Lazarevic MB, Hatta S, Hamm HE. 1994. *J. Biol. Chem.* 269:21519–25
230. Iiri T, Herzmark P, Nakamoto JM, Van Dop C, Bourne HR. 1994. *Nature* 371:164–68
231. Taylor JM, Jacob-Mosier GG, Lawton RG, Remmers AE, Neubig RR. 1994. *J. Biol. Chem.* 269:27618–24
232. Deleted in proof
233. Kawashima T, Berthet-Colominas C, Wulff M, Cusack S, Leberman R. 1996. *Nature* 379:511–18
234. Kraulis PJ. 1991. *J. Appl. Cryst.* 24:946–50
235. Bernstein FC, Koetzle TF, Williams JB, Meyer EF Jr, Brice MD, et al. 1977. *J. Mol. Biol.* 112:535–42